1 **Combining colour parameters and geochemical tracers to improve sediment source discrimination**

2 **in a mining catchment (New Caledonia, South Pacific Islands)**

3 Virginie Sellier[1] • Oldrich Navratil[2] • John Patrick Laceby[3] • Cédric Legout[4] • Anthony Foucher[1] •

4 Michel Allenbach[5] • Irène Lefèvre[1] • Olivier Evrard[1]

5 [1]Laboratoire des Sciences du Climat et de l'Environnement (LSCE), UMR 8212 (CEA/CNRS/UVSQ-IPSL),

6 Université Paris-Saclay, Gif-sur-Yvette (France)

7 [2] Laboratoire Environnement Ville Société (EVS), Université Lumière Lyon 2, UMR 5600 (CNRS), Lyon

8 (France)

9 [3] Alberta Environment and Parks, Calgary, Alberta (Canada)

10 [4]Institut des Géosciences de l'Environnement (IGE), UMR 5001, Grenoble (France)

11 [5]LIVE-EA 4243, Université de Nouvelle-Calédonie & LABEX Corail, Nouméa (Nouvelle-Calédonie,

12 France)

13 **Corresponding author:** selliervirg@free.fr ; Tel: (33)673910072

Abstract

Tracing the origin of sediment is needed to improve our knowledge of hydro-sedimentary dynamics at the catchment scale. Several fingerprinting approaches have been developed to provide this crucial information. In particular, spectroscopy provides a rapid, inexpensive and non-destructive alternative technique to the conventional analysis of the geochemical properties. Here, we investigated the performance of four multi-proxy approaches based on (1) colour parameters, (2) geochemical properties, (3) colour parameters coupled with geochemical properties and (4) the entire visible spectrum to discriminate sediment source contributions in a mining catchment of New Caledonia. This French archipelago located in the south-west Pacific Ocean is the world's sixth-largest producer of nickel. ~~Over the last century, human activities have induced significant land cover changes that have accelerated soil erosion processes around the world. In New Caledonia, a French island located in the south-west Pacific Ocean,~~ Oopen-cast nickel mining increases soil degradation and the downstream transfer of sediments in river systems, leading to siltation ~~of river systems. The~~ sediment sources considered in the current research were therefore sediment eroded ~~has raised many concerns regarding its impact on riverine systems (i.e. hyper sedimentation, overburden) and the island's ecosystems (i.e. flooding, lagoon siltation, water pollution).~~ from mining sub-catchments and non-mining sub-catchments. To this end,

~~.Indeed, spectroscopy measurements may provide important information on the spatial origin of sediment sources and their contributions~~

~~A sediment tracing study has been conducted to quantify the contribution of mining versus non mining sub catchments in one of the first areas exploited for nickel mining, the Thio River~~

~~catchment (397 km²).~~ ~~s~~Sediment deposited during two cyclonic events (i.e. 2015 and 2017) was collected following a tributary design approach in one of the first areas exploited for nickel mining on the archipelago, the Thio River catchment (397 km²). Source (n= 24) and river sediment (n= 19) samples were analyzed by X-ray fluorescence and spectroscopy in the visible spectra (i.e. 365-735 nm). ~~Four fingerprinting approaches based on (1) colour parameters, (2) geochemical properties, (3) colour parameters coupled with geochemical properties and (4) the entire visible spectrum were tested to estimate sediment source contributions.~~

The results demonstrated that the individual sediment tracing methods based on spectroscopy measurements (i.e. (1) and (4)) ~~did not provide sufficient discrimination~~ were not able to discriminate ~~between~~ sources. On the contrary, the geochemical approach (2) did discriminate sources with 83.1 % of variance in sources explained. However, it is the inclusion of colour properties in addition to geochemical parameters (3) which provides the strongest ~~provided the highest~~ discrimination between sources ~~–~~ with ~~(i.e.~~ 92.6 % of source variance explained~~)~~. For each of these approaches (2) and (3), the associated fingerprinting properties were used in an optimized mixing model. The predictive performance of the models was validated through tests with artificial mixture samples, i.e. where the proportions of the sources were known beforehand. Although with a slightly lower discrimination potential ~~(i.e. 83.1 % of variance explained in sources)~~, the ~~geochemical~~ 'geochemistry' ~~approach~~ model (2) provided similar ~~results~~ predictions of sediment contributions to those obtained with the coupled 'colour + ~~coupled with~~ geochemi~~cal~~stry' ~~approach~~ model (3). Indeed, the 'geochemistry' model (2) showed that mining tributary contributions dominated the sediments inputs with a mean contribution of 68 ± 25 % for the 2015 flood event whereas the 'colour + geochemistry' model (3) estimated that the mining tributaries contributed 65 ± 27 %. In a similar way, the contributions of mining tributaries were evaluated to 83 ± 8 % by the 'geochemistry' model (2) versus 88 ± 8 % by the 'colour + geochemistry' model (3) for the 2017 flood event. ~~In addition, mixed linear models associated with these two approaches have been experimentally validated with artificial mixture samples. The results obtained with model (3) showed that mining source~~

64 ~~contributions strongly dominated the sediments inputs with a mean contribution of 68% (SD 25%) for~~

65 ~~the 2015 flood event and 88% (SD 8%) for the 2017 flood event. These results suggest that~~

66 ~~catchment management should focus on the contributions of mining tributaries to reduce sediment~~

67 ~~inputs in the river systems.~~ Therefore, the use of these approaches based on geochemical properties

68 only (2) ~~and~~ or those coupled to colour parameters (3) ~~could~~ were shown to improve source

69 discrimination and to reduce uncertainties associated with~~precision of~~ sediment source

70 apportionment. These techniques could be extended to other mining catchments of New Caledonia

71 but also to other similar nickel mining catchments areas around the world~~.~~

72

73 **Keywords:** Nickel mining • Sediment source fingerprinting • Soil erosion • Modeling

74

1.Introduction

At the dawn of a fourth industrial revolution, demand for metalliferous minerals continues to increase and impact the world market (Prior et al., 2013;Highley et al., 2004). Currently, open-cast mining generates more than three-quarters of the world's metal ores. However, the extraction of these minerals is associated with deleterious impacts on the environment. In particular, these mines are responsible for the increase in soil erosion and the accelerated transfer of sediment in the river systems. Indeed, bare soil areas generated by mining activities including exploitation sites, prospection areas and access roads significantly increase runoff production (Yellishetty et al., 2013;Dumas et al., 2010;Abel et al., 2000). Moreover, the extraction of mineral ore is accompanied by a sharp production of mining wastes. Until the 1980s, no environmental regulation had been implemented to store this mining waste, and it was dumped directly onto the mountain slopes (Valette-Silver, 1993). Currently, this legacy mining waste provides an active source of sediment as it can progressively be remobilized (Coulthard and Macklin, 2003;James, 2013).

New Caledonia, an island located in the south-western Pacific Ocean and currently the world's sixth-largest producer of nickel, is in particular challenged with the problems of siltation of its river systems. Several studies outline how mining activities, which started in 1875, are generally responsible for these river morphological changes (Bird et al., 1984;Iltis, 1992;Garcin et al., 2017). In this case, excessive inputs of fine and coarse sediment triggered mainly during extreme rainfall events (e.g. cyclones and tropical depressions) have led to the disturbance of the sediment cascade in the river systems. A raising and widening of the riverbed has in particular been observed in the New Caledonian river systems by Garcin et al. (2017), leading to the increased occurrence of flooding events in these tropical regions. Owing to the occurrence of major cyclones in New Caledonia (i.e. on average one cyclone every 2.7 years (Garcin, 2010)), the local population regularly has to deal with the damage generated by these flood events: damage to human settlements, public infrastructure, agricultural land and human casualties. Moreover, suspended sediment is known to transport large

100 quantities of contaminants in river systems (Kumar and Maiti, 2015;Priadi et al., 2011;Varol, 2011).

101 Hedouin et al. (2007), and more recently Baudrimont et al. (2019), observed high concentrations of

102 trace metals, including Ni and Cr, in marine and freshwater organisms in New Caledonia. These

103 observations raise many questions about the health impact of mining activities on the populations

104 who eat a lot of fish. On a more global level, this anthropogenic activity also threatens the second

105 largest coral reef in the world, listed as a UNESCO World Heritage site (Davis and Fox, 2009). In

106 particular, the increased turbidity associated with sediment supply could disrupt coral metabolism

107 (i.e. photosynthetic processes) (Juillot, 2019). These coral reefs provide an exceptional biological

108 diversity and deliver several essential ecosystem services to the local population including fisheries,

109 coastal protection and tourism (Pascal, 2010). The implementation of effective and long-term

110 sediment control measures on mining sites (e.g. sediment retention basin, revegetation) is therefore

111 required to reduce sediment inputs into the lagoon. At this end, quantifying the sediment source

112 contributions from mining activities

113 becomes particularly important as the mining industries are subject to the "polluter pays" principle

114 applied since 1975, i.e. the obligation to fund remediation according to the extent of the damage

115 generated by mining activity on the environment (Clarke and David, 2010). Discriminating between

116 sediment sources generated by mining activities and other potential sediment sources is therefore a

117 real social, environmental, political and financial challenge in New Caledonia.

118 Indeed, other sediment sources that are not associated with mining activities as deforestation,

119 farming, pasture may contribute to sediment inputs in river systems. The use of fires to clear

120 landscapes also increases the area of bare soils (Dumas et al., 2010). Moreover, several invasive

121 species such as deers or wild pigs threaten soil stability through trampling and overgrazing (Shellberg

122 et al., 2010). Soils that are left uncovered with vegetation are more sensitive to erosion and they may

123 be exposed to landslides (Blake et al., 2009;Smith et al., 2011).

124   Sediment fingerprinting techniques have been developed since the 1970s to determine the

125   spatial origin of sediment sources and quantify their contributions (Klages and Hsieh, 1975;Walling et

126   al., 1979;Brown, 1985). These techniques are based on the analysis of multiple conservative

127   properties both in the sediments and their potential sources. The properties must necessarily be

128   conservative, i.e. the ranges of variation of these properties in the river material have to be

129   predictable based on those measured in the sediment sources. The ability of one or more of these

130   properties to discriminate between sources then allows to estimate the relative contribution of each

131   source through the use of a mixing model (Collins and Walling, 2002). Fallout radionuclides

132   (Wallbrink, 2004;Evrard et al., 2015;Wallbrink et al., 1998;Evrard et al., 2020), geochemical (Laceby

133   and Olley, 2015;Batista et al., 2018) and mineral properties (Gruszowski et al., 2003;Motha et al.,

134   2004) are the most frequently used tracers to quantify sediment source contributions. The use of

135   fallout radionuclides and geochemical properties as potential tracers was investigated to quantify the

136   sources of suspended sediment in the Thio River catchment (397 km²), one of the first catchments in

137   New Caledonia to be mined for nickel. Fallout radionuclides proved to be unsuitable (i.e. non-

138   discriminatory) while geochemical properties provided promising results, i.e. 83.1 % of variance

139   explained in sources (Sellier et al., 2019). The discrimination offered by geochemical properties was

140   particularly explained by the differences in geochemical composition outlined by Sevin (2014)

141   between the two dominant lithologies found in the archipelago: volcano-sedimentary formations

142   covering two thirds of the archipelago and peridotite massifs covering the remaining third where

143   mining activities are located. Mining erosion dominates 95 % of eroded areas identified on peridotite

144   massifs of the Thio River catchment according to the remote sensing study carried out by Garcin et

145   al. (2017). As a result, using geochemical properties is effective to indirectly quantify the sediment

146   contributions from mining activities and from areas devoid of mining activities. In this case, K

147   provides a straightforward tracer to discriminate the sediment sources (Sellier et al., 2019). Indeed,

148   volcano-sedimentary rock formations naturally contain high K elemental contents whereas peridotite

149   massifs are depleted in this element in New Caledonia (Sevin, 2014). Although these initial study

150 results were very promising, other less expensive, faster and possibly more efficient techniques than

151 the more conventional methods previously tested could be envisaged. For example, spectroscopy in

152 the mid-infrared (MIR) (Poulenard et al., 2009), the visible near-infrared (VNIR) and the shortwave-

153 infrared (SWIR) (Brosinsky et al., 2014) spectra have been used to quantify the sediment source

154 contributions. Spectroscopy is also non-destructive and requires low quantities of sample material.

155 Spectroscopy could therefore meet both the need for a simple, inexpensive, fast and portable

156 sediment tracing method in a context where flood events are frequent. This analysis technique could

157 also be more easily transferred to local populations so that they can carry out long-term

158 environmental monitoring of sedimentary contributions themselves.

159   Moreover, the geological specificity of the archipelago provides a strong contrast in terms of

160 soil colours observed either on the peridotite massifs or on the volcano-sedimentary formation rocks

161 and by extension, on the eroded sediments derived from these soils. On the one hand, the

162 weathering of peridotite massifs naturally enriched in Fe and transition metals such as Mn, Ni, Cr and

163 Co results in the formation of laterite profile composed of peridotites, saprolites, yellow laterites and

164 red laterites (from the bottom to the top). Hypermagnesian and ferrallitic ferritic soils that are rich in

165 goethite and hematite and that formed on the surface provide a particularly reddish-orange colour to

166 sediment derived from these exploited soils (i.e. mining sources, Figure 1) (Quantin et al.,

167 1997;Trescases, 1973). On the other hand, the weathering of volcano-sedimentary formation rocks

168 generates the formation of altered horizons rich in goethite and clay horizons rich in kaolinite (from

169 the bottom to the top) (Denis, 1988). The eroded sediment derived from fersialitic soils formed on

170 the surface is characterized by a yellow-grey colour (Figure 1). The differences made visually between

171 the two sources further encourage the analysis of sources by spectroscopy and especially

172 spectroscopy in the visible region of the spectrum (i.e. 365-735 nm). In particular, the colorimetric

173 parameters derived from the visible spectrum have been shown to be effective in discriminating

174 sediment sources. Their discrimination power has been tested both individually (Evrard et al.,

175 2019;Martínez-Carreras et al., 2010;Uber et al., 2019) and in combination with other tracers (e.g.

176 geochemical properties (Tiecher et al., 2015)) according to the conventional fingerprinting approach

177 (i.e. statistical analysis and use of a mixing model) (Collins et al., 1996). A more alternative approach

178 based on the entire visible spectrum with the partial least square regression (PLSR) models has also

179 been developed to trace origin of sediment sources in the literature (Legout et al., 2013;Tiecher et

180 al., 2015).

181

182 **Figure 1** Photographs of river material deposited on the channel banks of a mining tributary (left) and a
183 non-mining tributary (right) in the Thio River catchment

184 As part of this study, four sediment fingerprinting methods based on (1) colour parameters, (2)

185 geochemical properties, (3) colour parameters coupled with geochemical properties and (4) PLSR

186 models based on the whole visible spectrum were tested in the Thio River catchment. A tributary

187 design approach was implemented to trace the origin of sediments, i.e. sediment samples collected

188 on different tributaries were used as potential sources of the river sediment collected further

189 downstream on the Thio River (Laceby et al., 2017). Source (n=24) and river sediment (n=19) samples

190 were collected and analyzed by X-ray fluorescence and spectroscopy in the visible spectra (i.e. 365-

191 735 nm). For each of these sediment fingerprinting methods, the associated potential tracing

192 properties were used in an optimized mixing model. Tests with artificial mixture samples, i.e. where

193 the proportions of the sources were known beforehand were carried out to evaluate the predictive

194 performance of each model in order to select the best technique to be applied in the Thio River

195 catchment and possibly in other mining catchments of New Caledonia.

2.Materials and methods

2.1 Study area

Located in the southwestern Pacific Ocean, New Caledonia (18 500 km²) is made up of several islands, the largest of which is *La Grande Terre* (17 000 km²). The Thio River catchment (397 km²) is located on the east coast of this island (Figure 2-a). It has a mountainous relief, with an average altitude of 416 m above sea level (i.e. minimum: 0 m, maximum: 1392 m, Figure 2-a) and an average slope of 45 %. Two dominant lithologies are present in the catchment: volcano-sedimentary formations mainly located on the western part of the catchment and peridotite massifs concentrated in the eastern part of the catchment. Cherts (22 %), sandstone (9 %), a mix of basalt, dolerite and gabbro (6 %), polymetamorphic rocks (6 %) mainly constitute volcano-sedimentary formations whereas peridotite massifs are composed of laterites (18 %), peridotites (17 %), serpentines (10 %) and hazburgites (1 %) (Garcin et al., 2017) (Figure 1-b). The rock formation of these lithologies plays a key role in determining their degree of soil erodibility. In this case, Dumas (2010) described that volcano-sedimentary formations are less sensitive to soil erosion than peridotite massifs. Indeed, rocks from volcano-sedimentary formations such as basalts and cherts provide a certain resistance to erosion whereas laterites at the top of the profile are extremely sensitive to erosion processes, which explains why most forms of concentrated erosion (e.g. gullies, rills) and mass movements are mainly observed on peridotite massifs (Figure 3). However, the permanent vegetation covering 96 % of the Thio River catchment surface offers a relative protection against soil erosion across the catchment. Peridotite massifs naturally enriched in heavy metals have a low soil fertility, which explains why farming or pasture activities are not implemented on these soils (Quantin et al., 1997). Peridotite massifs have been exploited exclusively for their nickel resources since 1875. According to the mining registry, active and abandoned mining sites and exploration cover 21 % of the catchment area (Figure 2-c).

221   The Thio River catchment is subject to a tropical climate characterized by the alternation of a

222   hot wet season (November-April; mean temperature of 27 °C) and a cooler dry season (May-October;

223   mean temperature of 20 °C). The mean annual rainfall in the Thio River catchment is 1620 mm

224   despite strong seasonal fluctuations with the highest levels of precipitation recorded during the

225   cyclonic season between January and March (700 mm, 1981-2008; Alric (2009)). Although they only

226   occur on average once every 2.7 years, cyclones or tropical depressions may supply more than 20 %

227   of the annual rainfall in only one day according to local meteorological records (Météo France).

228

229   Twelve major tributaries flow into the main stem of the Thio River (28 km long) (Figure 2-b).

230   Ninety-two percent of the river channel length are characterized with slopes lower than 5 %.

231   According to Surell's classification (1841), the Thio River can be considered as torrential except in its

232   estuarine section. In addition, the longitudinal connectivity is exacerbated by the 8km² of bare soils

233   associated with past mining activities (~10 sites), ongoing mining operations (e.g. 2 sites: Thio

234   Plateau, Camps des Sapins) and the occurrence of 6 km² of mining roads. Bare soil areas increase soil

235   erosion processes on peridotites massifs, which once initiated, are difficult to contain (Figure3).

236   Heavy rainfall and the associated runoff exacerbate the widespread occurrence of rills, gullies,

237   landslides (Danloux and Laganier, 1991), thus contributing to connect the sediment sources to the

238   tributaries and consequently to the main river (Figure 3). For low intensity floods (i.e. <200 $m^3.s^{-1}$), a

239   strong remobilization of sediments in New Caledonian river systems has been observed (Allenbach et

240   al., 2020), thereby indicating that a lateral connectivity occurs in the Thio River catchment through

241   the occurrence of channel bank erosion.

242

243

a.

b.

c.
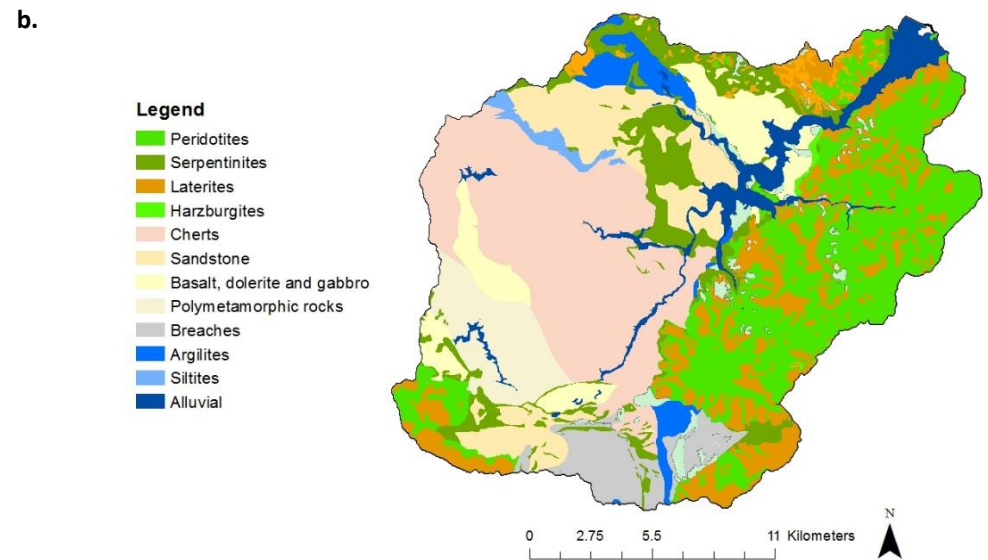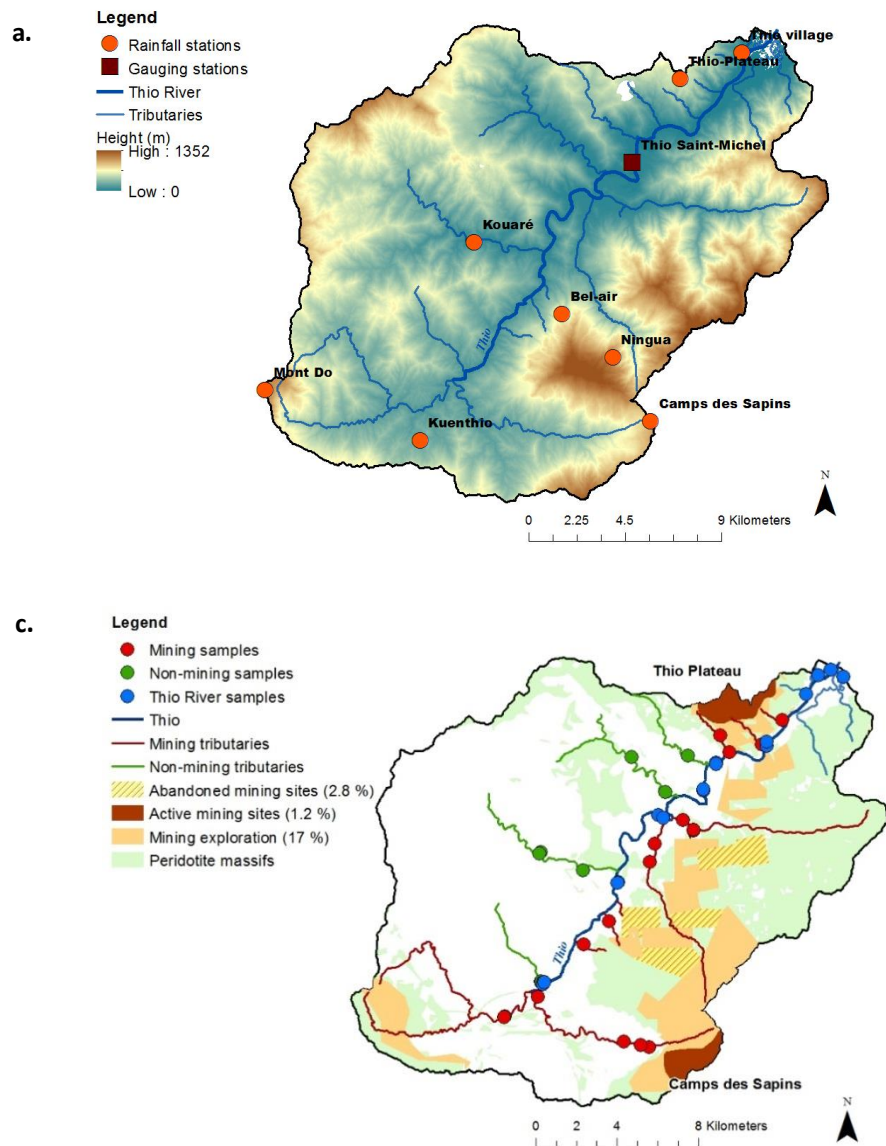
Figure 2 Location of the rainfall and river monitoring stations (a), main lithologies (b) and location of the sediment samples collected along with tributary source classifications (c) conducted in the Thio River catchment, New Caledonia

245

246

Figure 3 Photographs of concentrated erosion and mass movement processes observed on peridotite massifs of the Thio River catchment

2.2 Hydro-sedimentary monitoring

Three rainfall stations (Thio Plateau, Thio village, Camps des Sapins; Figure 2-b) are operated by Météo France and five others are managed by the DAVAR (Direction des Affaires Vétérinaires Alimentaires et Rurales; i.e. Kouaré, Bel-Air, Ningua, Kuenthio, Mont Do), with daily records available since 1952 for some stations (e.g. Thio village). Daily discharge has been monitored at a river gauging station located on the main stem of the Thio River (at Saint-Michel) since 1981 by the DAVAR (Figure 1-a).

2.3 Sources and river sediment sampling

In this study, two extreme events were investigated: Cyclone Murcia on February 25, 2015 and Cyclone Cook on April 10, 2017. These cyclones respectively contributed to 7 % of annual rainfall in 2015 and 25 % in 2017. They generated floods with a return period of 10 years (i.e. 3500 $m^3.s^{-1}$). To trace the origin of sediment, lag deposits were collected as an alternative of suspended sediment sampling on channel bars of mining tributaries (n= 16), non-mining tributaries (n= 8) and the Thio

262 River (n= 19) according to the tributary design approach recommended by Laceby et al. (2017)

263 (Figure 2-c). Lag deposits ~~They~~ were sampled after the two major floods generated by Cyclone

264 Murcia (n= 31) and Cyclone Cook (n= 12). These two sample sets were respectively sampled between

265 April 30 and May 5, 2015 and between May 16 and 17, 2017. At each sampling site, five to ten

266 subsamples of fine sediment were collected depending on the amount of observed sedimentary

267 material. They were sampled across a 10 m² surface with a plastic trowel at exposed subaerial sites

268 free of vegetation on channel bars. The subsamples were composited into one sample representative

269 of the fine sediment deposited on the channel bars. The samples were oven-dried at 40°C for ~48

270 hours. Particle size selectivity may occur during the erosion, transport and deposition processes

271 inducing an overall finer particle size distribution in the river material compared to the sources. This

272 selectivity can lead to a non-conservation of the fingerprinting properties. For example, certain

273 properties are preferentially contained in a given particle size fraction which can create a relative

274 enrichment or conversely a relative depletion of these properties in the river material according to

275 the particle size fraction analyzed. In order to avoid this particle size effect, river sediment and

276 source samples were sieved to 63 μm, which is the most commonly used fraction in sediment tracing

277 research (Owens and Walling, 2002;Navratil et al., 2012).

278   **2.4 Preparation of artificial mixture samples**

279   Equal quantities of all mining tributary samples (0.4g for each sample, n= 16) were mixed

280 together to create a composite sample which would have an overall geochemical and colour

281 signature of the mining sources in the Thio River catchment (i.e. 'Mining source' pole). The same

282 process was carried out with non-mining tributary samples (0.4g for each sample, n= 8, 'Non-mining

283 source' pole). 'Mining source' and 'Non-mining source' pole samples were then mixed in known

284 proportions to create artificial mixture samples (n= 21, 0-100 % with a 5 % step, Table 1).

285

286 **Table 1** Proportions of mining and non-mining sources (%) in artificial mixture samples (M_i). *M6 was withdrawn*

287 *from this study because an error occurred at the time of its completion (not consider in the study).*

M_i	Proportions of 'mining source' pole (%)	Proportions of 'non-mining source' pole (%)
M1	0	100
M2	5	95
M3	10	90
M4	15	85
M5	20	80
M6	*25*	*75*
	(not consider in the study)	*(not consider in the study)*
M7	30	70
M8	35	65
M9	40	60
M10	45	55
M11	50	50
M12	55	45
M13	60	40
M14	65	35
M15	70	30
M16	75	25
M17	80	20
M18	85	15
M19	90	10
M20	95	5
M21	100	0

288

2.5 Source, river sediment and artificial mixture sample analyses

290   Spectroscopy measurements in the visible were carried out with a portable diffuse reflectance

291 spectrophotometer (Konica Minolta 2600d) at the Institut des Géosciences de l'Environnement (IGE,

292 Grenoble, France). To this end, between 0.1 g and 4 g of Thio River sediment (n= 19), source (n= 16)

293 and artificial mixture samples (n= 20) were stored in 60 mL polystyrene tubes. In order to perform

294 the analyses, the spectrophotometer was installed on a flat surface with the measuring window

295 facing upwards. The tubes were then placed on the 3-mm radius circle measuring cell. Because of the

296 rather small measuring area and to take into account the possible heterogeneity within the samples,

297 three measurements were carried out on river sediment and sources samples for each tube. For

298 artificial mixture samples, the experimenter who conducted the analyses performed four

299 measurements. Spectral reflectances were measured between 365 nm and 735 nm with a 10-nm

300 resolution. Several parameters were applied for each measurement: D65 illuminant, 10° angle

301 observer and specular component excluded. Raw data collected corresponds to the spectral

302 reflectance percentage for each of the 39-wavelength classes. From these raw data, 15 variables of

303 various colorimetry models were derived. Among these components, XYZ tri-stimulus values were

304 calculated based on the colour-matching functions defined by the International Commission on

305 Illumination (CIE 1931). The standardized tri-stimuli were then converted into CIELab and CIELu'v'

306 cartesian coordinate systems using the equations provided by CIE (1976) and then into CIELch,

307 CIEL*a*b* cartesian coordinate systems using the equations provided by CIE (1994) (Rossel et al.,

308 2006). First Derivative reflectance of the Visible Spectra (FDVS) of each sample was also derived from

309 the initial reflectance spectrum. According to Tiecher et al. (2015), the use of FDVS avoids differences

310 in baseline positions and allows to get rid of the small differences due to uncontrolled sources of

311 variation, as sample packaging. A zero and a white calibration were performed before each set of

312 measurements. In addition, and in order to evaluate a potential drift of the device's signal, control

313 measurements were carried with red, green, yellow panels and three contrasted sediment samples

314 before and after each set of measurements.

315 Measurements of 11 geochemical elements (i.e. Mg, Al, Si , K, Ca, Ti, Cr, Mn, Fe, Ni and Zn) on

316 the samples were conducted by pre-calibrated energy dispersive X-ray fluorescence spectrometry

317 (Epsilon 3, Malvern PANalytical) with certified reference samples including Internal Atomic Energy

318 Agency (IAEA) standards. Correlations between the determined and the standard elemental contents

319 were comprised between 0.90 and 0.99. The associated mean relative error was 9 % (SD 8 %).

320 Between 0.2 and 0.5 g of the samples were packed in small mass holder (SMH) cells with an air

321 double X-ray Mylar film and analyzed at the Laboratoire des Sciences du Climat et de

322 l'Environnement (LSCE, Gif-sur-Yvette, France). Samples were irradiated with a primary beam

323 generated by an Rh anode X-ray tube emitting electromagnetic waves between 100eV and 1MeV

324 with a maximum power, typical current and voltage fixed to 15 W, 3mA and 50 kV respetively. The

325   associated Si-drift detector had a Be window thickness of 8 μm and recorded the sample spectrum in

326   a 2D optical geometry configuration. X-ray intensities were converted into concentrations using the

327   Epsilon 3 software program through the application of the fundamental parameters method.

328   **2.6 Statistical analysis and sediment tracing**

329   2.6.1   Conventional mixing model

330   In general, the sediment source fingerprinting approach is composed of four main steps: (1)

331   range test, (2) the Mann-Whitney U test, (3) a stepwise discriminant function analysis and (4) a

332   mixing model (Collins et al., 1996;Laceby and Olley, 2015). For the range test, all variables exhibiting

333   values in the river sediment samples that were outside of the range found in the potential sources

334   (i.e. between the minimum and maximum values found in source samples) were excluded from the

335   analysis. It is important to restrict the tracing parameters to those that show a conservative behavior

336   to avoid incorrect source prediction and consequently inaccurate estimations of source contributions

337   (Sherriff et al., 2015). Thereafter, the Mann-Whitney U test (α= 0.05, p-value <0.01) was performed

338   to evaluate whether ~~remaining~~ conservative variables could discriminate ~~the source~~mining tributary

339   samples versus non-mining tributary samples. A stepwise discriminant function analysis (DFA) was

340   independently run on three set of potential tracing properties: (1) colour parameters (i.e. 'colour'),

341   (2) geochemical properties (i.e. 'geochemistry') and (3) colour parameters and geochemical

342   properties (i.e. 'colour + geochemistry'). For the last set, the raw values of the variables were

343   normalized in order to make them comparable. Indeed, several colour parameters were within an

344   order of magnitude of around 0.01 whereas for the geochemical parameters the difference was

345   around 10^6 mg kg^{-1} which resulted in a poorly conditioned matrix for the DFA.

346   The following calculation was therefore applied on the variable values to normalize them: x_i –

347   x_{min}/ x_{max} - x_{min} where xi was value found in source sample (i), x_{min} and x_{max} were respectively the

348   minimum and maximum values found in the source samples. The DFA was carried out to select the

349   optimal number of potential tracers to discriminate the sources for each modelling approach with

350   the optimal number of potential tracers which must provide the lowest Wilks' lambda value from

351   analysis of variance. Indeed, the closer the Wilks' lambda value is to 1, the lower the variability within

352   the sources compared to the total variability. The DFA was performed in the backward mode with a p

353   >0.01 used to select a tracer and p <0.01 used to remove a tracer. The *Statistica* software was used

354   to carry out the DFA because it has the advantage of automatically identifying and eliminating

355   collinear variables.

356   Finally, a classical solver-based mixing model was used to model the source contributions from

357   the mining and non-mining tributaries to target sediment through simultaneously minimizing the

358   mixing model difference (MMD) (Evrard et al., 2019):

$$MMD = \sum_{i=1}^{n}((C_i - (A_i x + B_i(1-x))/C_i) \quad Equation\ 1$$

359   where n is the number of parameters in the model chosen by the selection process (i.e. steps 1, 2, 3);

360   C_i is the Thio River sediment sample parameter (i); x and (1-x) were respectively the contributions of

361   source A and B (i.e. mining and non-mining tributaries); A_i is the mean of parameter (i) in source A

362   and B_i is the mean of parameter (i) in source B. The proportional contribution from each source (x)

363   was modelled by solving Equation 1 with the Solver Function in Microsoft Excel with x being between

364   0 and 1 and the sum of source contributions (i.e. x and 1-x) equaling 1. The GRG Non-Linear solving

365   method was used with automatic scaling in Solver, ignoring integer constraints, with a maximum run

366   time of 5000 and allowing for 2500 iterations. For each of the 2500 iterations, the values of the

367   variables were determined randomly with respect to their initially fixed ranges of values. A constraint

368   precision and convergence of $1.0\ 10^{-6}$ were selected for each of the model runs. To test the reliability

369   of the 'colour', 'geochemistry' and 'colour + geochemistry' models, these latter were tested on

370   artificial mixture samples.

| 371 | 2.6.2   FDVS- PLSR model |

372   FDVS-PLSR models were built following the methodology described in Poulenard et al. (2012).

373 The first step consisted in applying a principal component analysis (PCA) to evaluate the overall

374 variability between FDVS (i.e. 38-wavelength class) of source samples. Subsequently, a discriminant

375 analysis (DA) was conducted based on the PCA scores. The purpose of this analysis was to compare

376 the Mahalanobis distance between sources samples and to determine if FDVS of source samples

377 could discriminate the sources. Relationships between FDVS (x variate) and the corresponding weight

378 contribution of the sediment source data sets (y variate) were analyzed using PLSR. The PLSR models

379 were carried out based on the component set providing the lowest predictive error (PRESS, option on

380 XLStat software). Two independent PLSR models were built to estimate the two sediment source

381 contributions. As the artificial mixtures were measured four times by spectroscopy, 84 FDVS of

382 artificial mixture samples were generated including 50 values that were randomly selected to build

383 the models (training set (ST)) and 34 to validate the models (validation set (SV)). The SV:ST ratio used

384 was approximately 1:2, which is in agreement with recommendations provided in the literature

385 (Daszykowski et al., 2002). To evaluate the performance of PLSR models, several indicators such as

386 coefficient of linear regression (r^2), root mean square error of calibration (RMSEC) and root mean

387 square error of prediction (RMSEP) values were calculated. Unlike the conventional fingerprinting

388 approach, the estimated contributions of sources were not limited to be in the range of 0 % and 100

389 %. In a similar way, the sum of source contributions was not constrained to be equal to 100 %. As a

390 result, another way to control the reliability of predictions was to sum the prediction proportions of

391 both models (Legout et al., 2013). FDVS of river sediment samples were then introduced into these

392 PLSR models to estimate the contribution of sediment sources.

393   **3.Results**

394   **3.1 Source description**

395   The ranges of values of all colour parameters measured in the Thio River sediment samples

396   systematically plotted within the range of values observed in the two potential sources (i.e. mining

397   and non-mining tributaries; Figure 4 and Table 2). The range test results confirmed the conservative

398   character of these parameters. For geochemical properties, elemental concentrations measured in

399   the river sediment also plotted within the range of concentrations found in sources (Sellier et al.,

400   2019). In similar way, the range tests applied on geochemical properties showed that all these

401   properties were also conservative.

402
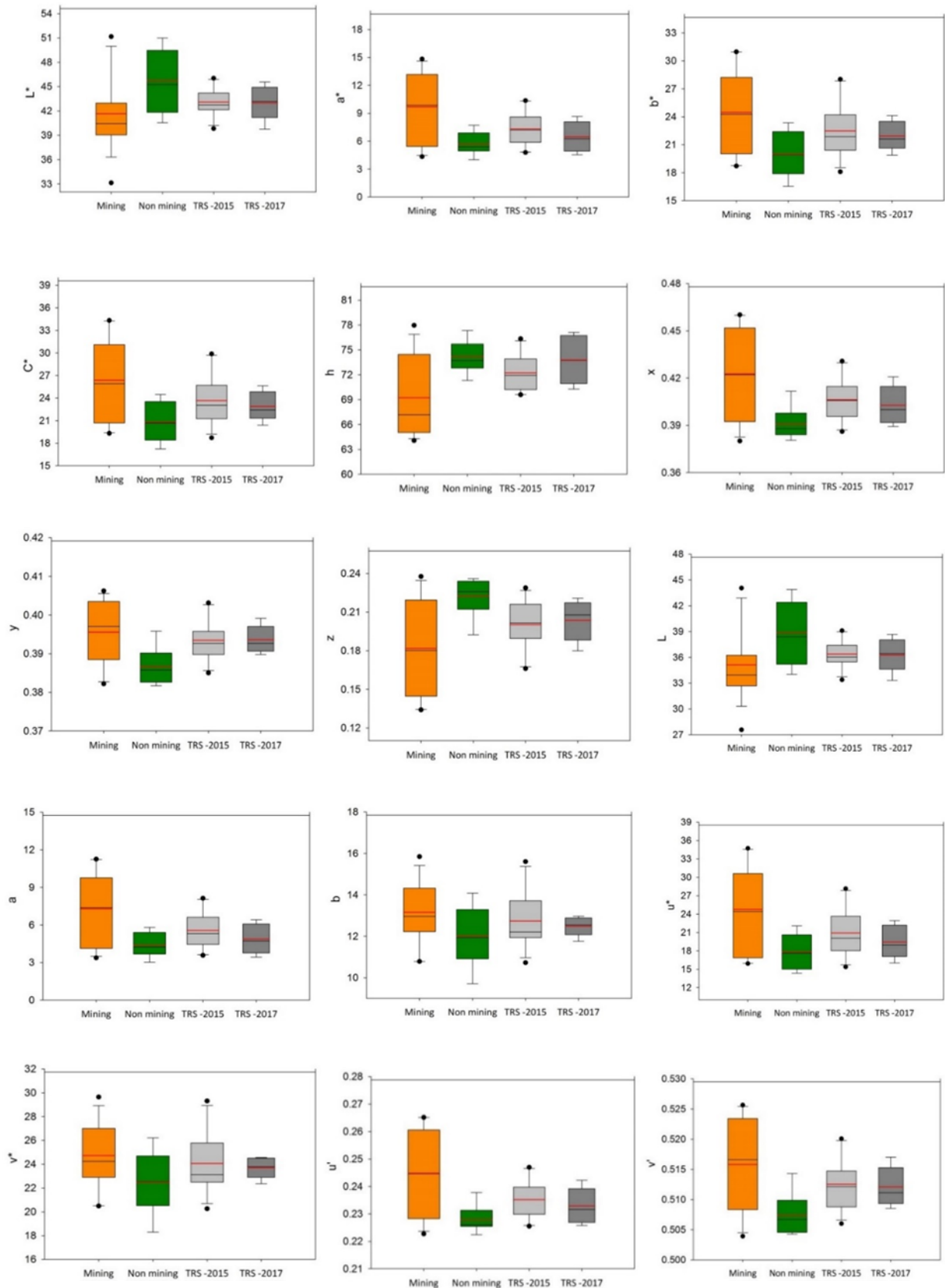
Figure 4 Box-plots of colour parameter values in the <63 µm fraction of sediment collected on the mining tributaries (Mining), non-mining tributaries (Non-mining) and the main Thio River (Thio River sediment (TRS)-flood events of 2015 and 2017). The box indicates the location of the first and third quartiles; the black line indicates the median value; the red line indicates the mean value

Table 2 Mean values of geochemical element contents and colour parameters in the <63 μm fraction of sediment sources and Thio River sediment (SD: standard deviation); results of Mann-Whitney U test and individual DA used to identify the potential tracers to differentiate sources supplying sediment to the Thio River

Fingerprinting property	Mann-Whitney U test *Mining tributaries versus non-mining tributaries*		DA- correctly classified samples (%)	Mean ± SD			
	U-value	p-value		Mining tributaries (n= 16)	Non-mining tributaries (n= 8)	Thio River sediment 2015 (n= 11)	Thio River sediment 2017 (n= 8)
Geochemical tracers							
Al *(g kg⁻¹)*	8	0.000	87.5	21 ± 21	67 ± 8	43 ± 15	29 ± 6
Ca *(mg kg⁻¹)*	21	0.007	62.5	3731 ± 470	9286 ± 5194	5281 ± 1201	3945 ± 666
Cr *(mg kg⁻¹)*	124	< 0.0001	83.3	7480 ± 4606	706 ± 967	4359 ± 2185	5715 ± 1786
Fe *(g kg⁻¹)*	121	0.000	91.6	144 ± 70	62 ± 24	43 ± 15	29 ± 6
K *(mg kg⁻¹)*	2	< 0.0001	95.8	1657 ± 2160	14019 ± 3702	5944 ± 3294	3750 ± 974
Mg *(g kg⁻¹)*	119	0.000	83.3	99 ± 59	16 ± 13	88 ± 33	117 ± 21
Mn *(mg kg⁻¹)*	108	0.006	83.3	2531 ± 1317	1439 ± 606	2068 ± 667	1786 ± 516
Ni *(mg kg⁻¹)*	125	< 0.0001	91.6	6576 ± 5075	358 ± 339	4218 ± 1938	4341 ± 1239
Si *(g kg⁻¹)*	6	< 0.0001	91.6	178 ± 42	254 ± 28	221 ± 15	204 ± 7
Ti *(mg kg⁻¹)*	13	0.001	87.5	1409 ± 2077	5446 ± 835	2771 ± 1197	1663 ± 457
Zn *(mg kg⁻¹)*	68	0.834	-	146 ± 47	125 ± 4	134 ± 17	125 ± 8
Colour parameters							
L*	24	0.013	-	41.6 ± 4.6	45.7 ± 3.9	43.1 ± 1.7	43.0 ± 2.0
a*	104	0.013	-	9.7 ± 3.8	5.7 ± 1.2	7.3 ± 1.9	6.5 ± 1.7
b*	106	0.009	70.8	24.5 ± 4.5	20.0 ± 2.5	22.5 ± 3.0	21.9 ± 1.6
C*	108	0.006	66.6	26.4 ± 5.5	20.8 ± 2.7	23.7 ± 3.5	22.9 ± 2.0
h	26	0.019	-	69.2 ± 4.8	74.2 ± 1.9	72.2 ± 2.2	73.8 ± 2.9
x	107	0.007	75	0.42 ± 0.03	0.39 ± 0.01	0.41 ± 0.01	0.40 ± 0.01
y	111	0.003	79.2	0.396 ± 0.008	0.387 ± 0.005	0.393 ± 0.005	0.394 ± 0.004
z	19	0.005	75	0.18 ± 0.04	0.22 ± 0.01	0.20 ± 0.02	0.20 ± 0.02
L	27	0.013	-	35.1 ± 4.2	38.9 ± 3.7	36.4 ± 1.6	36.3 ± 1.9
a	103	0.016	-	7.3 ± 2.9	4.4 ± 1.0	5.6 ± 1.5	4.9 ± 1.2
b	91	0.106	-	13.1 ± 1.5	12.0 ± 1.5	12.7 ± 1.4	12.5 ± 0.4
u*	101	0.023	-	24.8 ± 6.9	17.8 ± 2.8	20.9 ± 4.0	19.4 ± 2.7
v*	93	0.081	-	24.7 ± 2.8	22.5 ± 2.7	24.1 ± 2.6	23.7 ± 0.8
u′	105	0.011	-	0.245 ± 0.016	0.228 ± 0.005	0.235 ± 0.007	0.233 ± 0.007
v′	111	0.003	79.2	0.516 ± 0.008	0.507 ± 0.004	0.513 ± 0.004	0.512 ± 0.003

3.2 Selection of parameters/properties for modelling

3.2.1 'Colour' model

According to the Mann-Whitney U test results, six colour parameters (*i.e.* b*, C*, x, y, z, v') provided significant discrimination between the two sediment sources (*i.e.* p-value < 0.01, Table 2). The backward DFA selected only v' as the optimal tracer of mining and non-mining source sediments (Figure 4, Table 3). Although this parameter correctly classified 79.2 % of sources, the high Wilk's lambda value obtained (i.e. 0.7209, Table 3) induced that only 27.9 % of variance was explained by v'. The low Mahalanobis distance value obtained (i.e. 1.6) confirmed that sediment sources were not well separated. Accordingly, and owing to the high error percentage of the source discrimination provided by this approach (i.e. 72.1 %), source contributions were not modeled with the 'colour' model.

3.2.2 'Geochemistry' model

When considering the two potential sediment sources, all geochemical properties (except Zn) were selected as potentially discriminant by the Mann-Whitney U test (i.e. p-value < 0.01, Table 2). Among the 10 potential tracers, K was selected by the backward DFA to model sediment source contributions from mining and non-mining tributaries with 95.3 % of sources correctly classified and 83.1 % of variance explained by K. This percentage of variance explained was deduced from the final Wilk's lambda value obtained (i.e. 0.1691). Moreover, the Mahalanobis distance value showed that the sediment sources were well separated from each other with a significant distance of 20.3 (Table 3) (Sellier et al., 2019).

3.2.3 'Colour + geochemistry' model

When combining colour parameters and geochemical properties, the DFA selected five optimal tracers (i.e. K, Ca, Ti, b*, C*) able to correctly classify 100 % of the sources. A significant improvement in the source discrimination was observed with the lowest Wilk's lambda value obtained (i.e. 0.0734)

and the highest percentage of variance explained (i.e. 92.6 %). Moreover, the Mahalanobis distance value obtained (i.e. 52.1) was more than 2.5 times higher than that estimated with the 'geochemistry' model (Table 3), thus resulting in a better separation between sediment sources than the previous approach (i.e. 'geochemistry')

Table 3 Results of DFA used to identify the optimum tracer combination to differentiate sources supplying sediment to the Thio River

Fingerprint property selected	Wilks'Lambda	Variance explained by the variables (%)	Squared Mahalanobis distance	Correctly classified samples (%)
'Colour'				
v'	0.7209	27.9	1.6	79.2
'Geochemistry'				
K	0.1691	83.1	20.3	95.3
'Colour + Geochemistry'				
K, Ca, Ti, b*, C*	0.0734	92.6	52.1	100

3.3 Assessment of model performance on artificial mixture samples

Prior to applying mixing models to river sediments, preliminary tests were conducted to control the validity of the models (i.e. 'geochemistry' and 'colour + geochemistry') and the associated estimations of source contribution errors. When applying these models on the artificial mixture samples, actual and predicted proportions were well correlated for both models (i.e. r^2= 0.99 and r^2= 0.98 respectively for 'geochemistry' and 'colour + geochemistry' models, SD_{max} = 3 %) (Figure 5).

However, the 'geochemistry' model described in Figure 5-a showed that the contributions of mining tributaries were overestimated. With 100 % of actual mining contributions, 100 % of mining contribution was predicted by the model. However, instead of 0 % of actual mining contributions, a mining contribution of 15.5 % was predicted by the model. In other words, ~~t means that~~ the more the estimated mining source contributions tends towards 0 %, the greater the associated

overestimation (i.e. maximum 15.5 %) (Figure 5-a). The 'colour + geochemistry' model also provided a slight overestimation of the contribution of mining tributaries (i.e. 7 % intercept of the regression line, Figure 5-b). Given the slope of the regression line calculated is close to 1 (i.e. 0.98), this 7 % overestimation remains constant over the entire range of potential contributions.
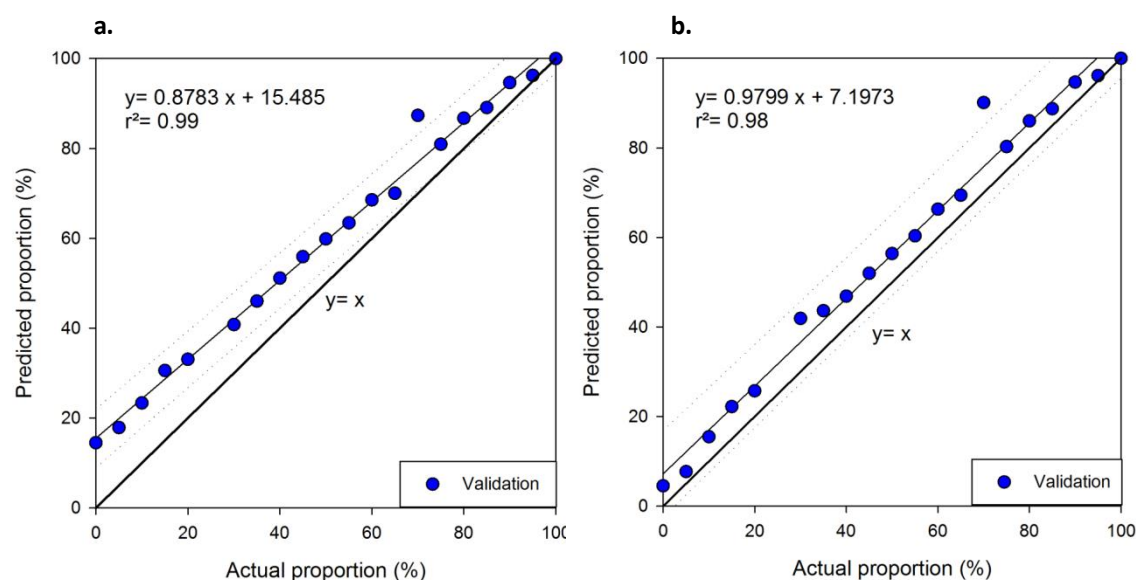
Figure 5 Comparison between actual mining source proportions prepared in artificial mixtures and the mining source proportions predicted by the 'geochemistry' (a) and 'colour + geochemistry' (b) models

3.4 Building partial least-squares models based on FDVS

Mining sources are characterized by a red-orange color while sediments originating from non-mining sources are yellow-grey colour (Figure 1). The colour contrasts may be explained by the distinct geochemical composition of these sources. Mean FDVS indicated the presence of goethite (i.e. at 445 and 525 nm), hematite (i.e. at 555, 565 and 575 nm), and organic matter (i.e. between 600-700 nm) (Debret et al., 2011) in both mining and non-mining sources (Figure 6). In similar way, the Thio River sediment samples (2015, 2017) showed similar characteristics since the variations of the mean FDVS remained between those found in the sources (Figure 6). Nevertheless, some differences can be observed between the sources. The spectral signature of goethite is slightly stronger at 445 nm in non-mining tributaries compared to mining tributaries. No difference between sources was observed at 525 nm, the second wavelengths characterizing the presence of goethite. In

470 contrast, the spectral signature of hematite (*i.e.* at 555, 565 and 575 nm) was stronger in mining

471 tributaries than in non-mining tributaries.
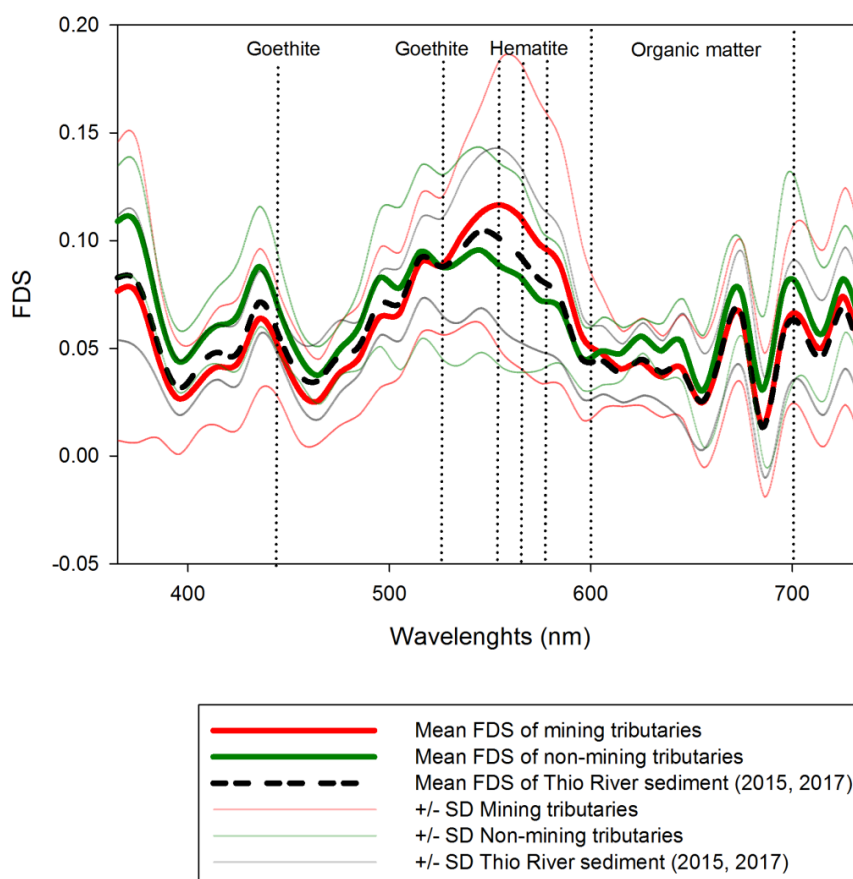
472 **Figure 6** FDVS measured in the <63 µm fraction of sources and Thio River sediment samples

473 To test the potential discrimination offered by FDVS, a PCA was applied on the source data set.

474 The first ten principal components from PCA explained 99 % of the total variation in the spectra. The

475 DFA performed on these components resulted in a final Wilks' lambda value of 0.1585. In other

476 words, t means that 84.1 % of variance is explained by these ten components. Moreover, 100 % of

477 the source samples were correctly classified. The performances of FDVS-PLSR models are presented

478 in Figure 7. The mining and non-mining tributary FDVS-PLSR models provided an excellent correlation

479 between actual and predicted proportions with r^2 and slopes close to 1 and intercepts of linear

480 regression close to 0. The root mean square error of calibration (RMSEC) values estimated for both

481 models were low, i.e. 3.4 % and 3.1 % respectively for mining (Figure 7-a) and non-mining tributary

482   models (Figure 7-b). These models also provided a good predictability of source contributions with

483   low root mean square error of prediction (RMSEP) values (i.e. 8.0 % and 4.7 % respectively for mining

484   and non-mining tributary models). Another way to control the reliability of predictions was to sum

485   the predicted proportions of both models (Legout et al., 2013). Considering the whole data set used

486   in the construction of the partial least-squares regression models (i.e. calibration and validation) led

487   to a mean sum of the predicted source proportions of 102 % (SD 3 %, range: 98-114 %), thus

488   highlighting the effective prediction performance of FDVS-PLSR models.
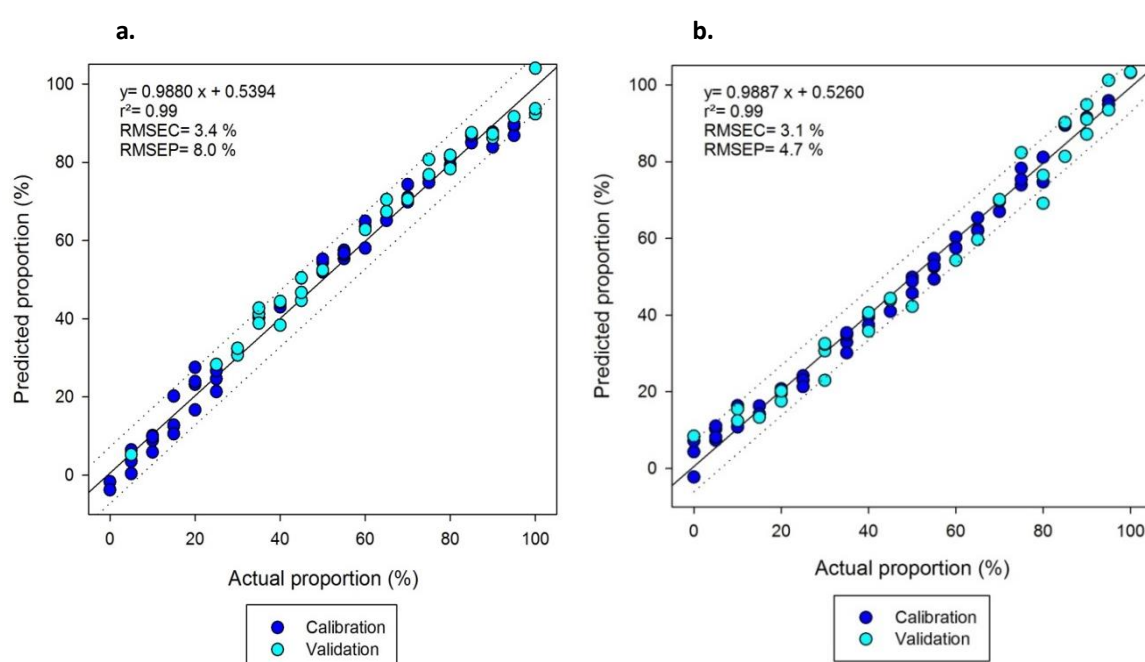
489   **Figure 7** Building of FDSV-PLSR models for mining sources (a) and non-mining sources (b)

490   **3.5 Source apportionment modelling**

491   3.5.1   'Geochemistry' model

492   The 'geochemistry' model estimated that the mining tributaries contributed an average of 65

493   ± 27 % of the Thio River sediment during the 2015 flood event; they therefore dominated sediment

494   inputs overall during this event. Nevertheless, non-mining tributaries mainly contributed to the

495   sediment inputs at three sampling points along the Thio River (Figure 8-a, Table 4, sampling points [3,

496   5, 7]). These contributions did not, however, compensate for those provided by mining tributaries in

497   the estuary (63-89 %). Indeed, the dominant mining contributions found in upstream river reaches

498   (96 %, Figure 8-a, Table 4, sampling point [1]) gradually decreased along the Thio River, fluctuating

499   between 17-77 % before increasing again at the confluence between the Thio River and the mining

500   tributaries draining the Thio Plateau mining area (i.e. 85 %, Figure 8-a, Table 4, sampling point [8])

501   and reaching 60-64 %.

502

503   The 'geochemistry' model also demonstrated that mining tributaries dominated sediment

504   inputs with a mean contribution of 83 ± 8 % during the 2017 flood event (Table 5). The lowest mining

505   tributary contributions estimated (i.e. 69 %) was found after the confluence with the Kouaré non-

506   mining tributary (Figure 8-b, Table 5, sampling point [4]). Nevertheless, further downstream, the

507   proportions of the mining sources increased again to reach 77-83 % in the estuary (Figure 6-b, Table

508   5, sampling points [7, 8]).

509
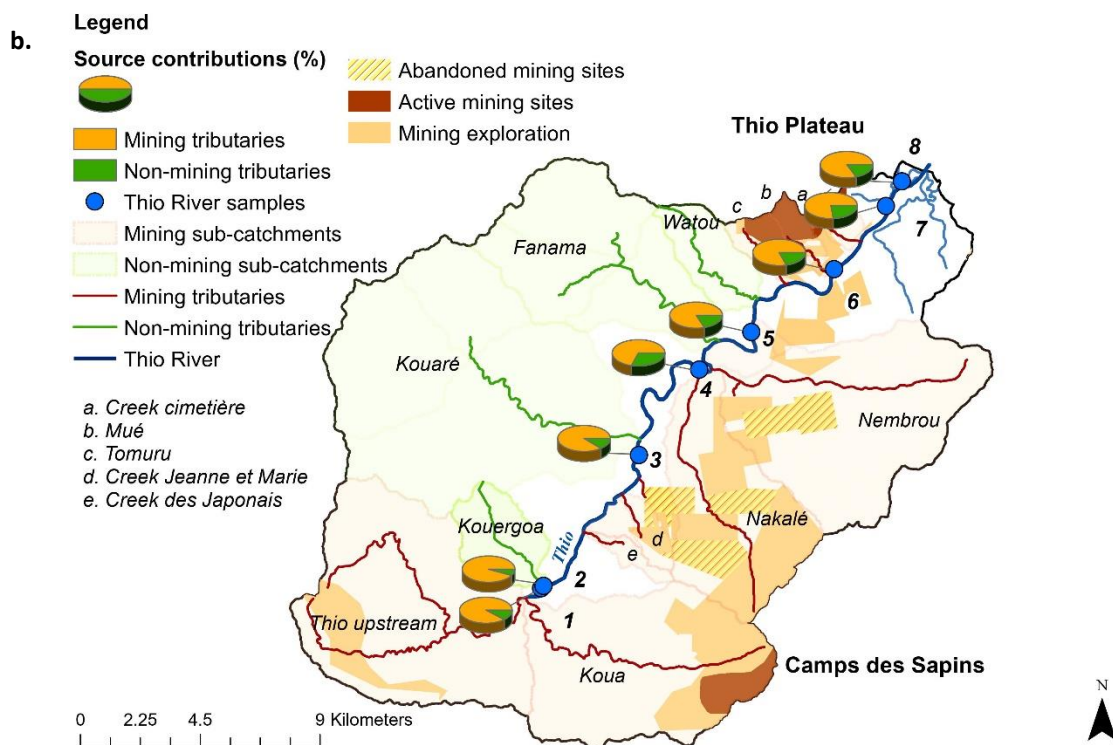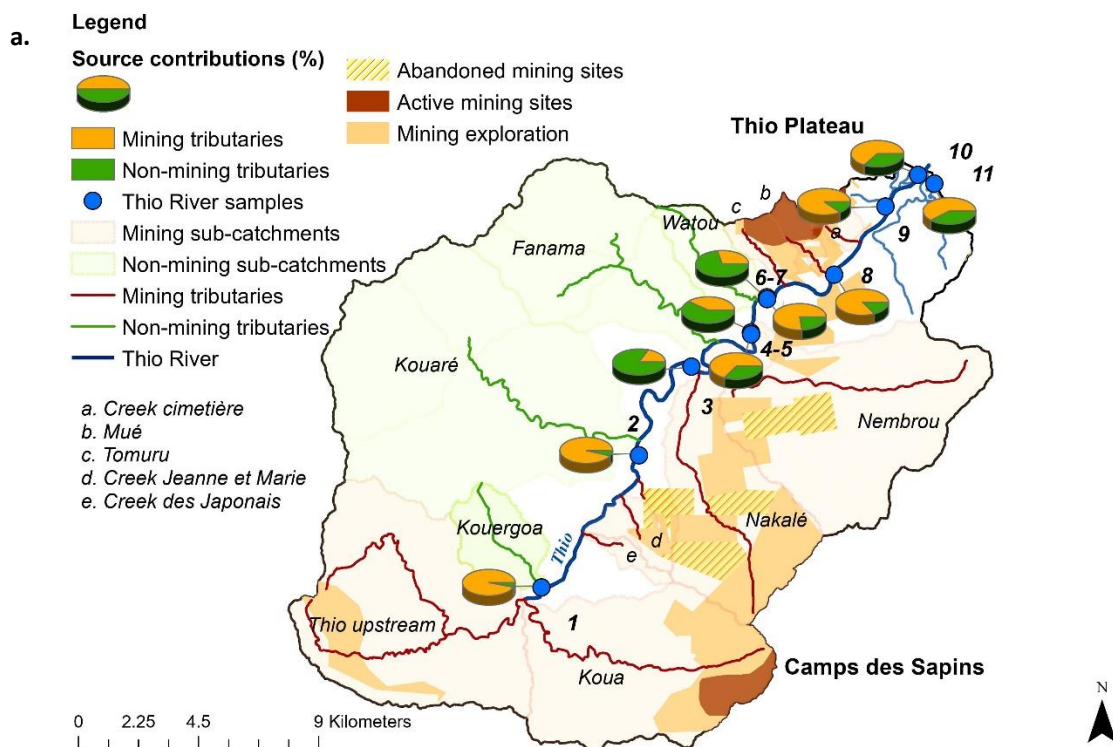
Figure 8 Relative contributions of mining and non-mining tributaries to the sediment collected in the Thio River during the 2015 (a) and 2017 (b) flood events using the 'geochemistry' model

516   3.5.2   'Colour + geochemistry' model

517   Similar results were obtained with the 'colour + geochemisty' model. The contributions of

518   mining tributaries were estimated to an average of 68 ± 25 % for the 2015 flood event. Mining

519   tributary contributions provided almost all the sediment transiting the uppermost reach of the Thio

520   River (i.e. 99 %, Figure 9-a, Table 4, sampling point [1]). However, after the confluence with the

521   Kouaré tributary, non-mining tributaries dominated with a contribution of 83 % (Figure 9-a, Table 4,

522   sampling point [3]). Further downstream, the contribution of mining tributaries increased again with

523   supplies varying between 34- 89 % to reach 58- 70 % in the estuary (Figure 9-a, Table 4). The largest

524   difference between 'geochemistry' and 'colour + geochemistry' model outputs was 18 % for the 2015

525   flood event.

526   The 'colour + geochemistry' model also demonstrated that 88 ± 8 % of the sediment supply

527   originated from mining tributaries during the 2017 flood event. Along the Thio River, mining tributary

528   contributions varied between 100 % in the uppermost reach, 74 % after the Kouaré river confluence

529   and 83-85 % in the estuary (Figure 9-b, Table 5). The largest difference between 'geochemistry' and

530   'colour + geochemistry' model outputs was 10 % for the 2017 flood event (Table 5).

531

532

533

534
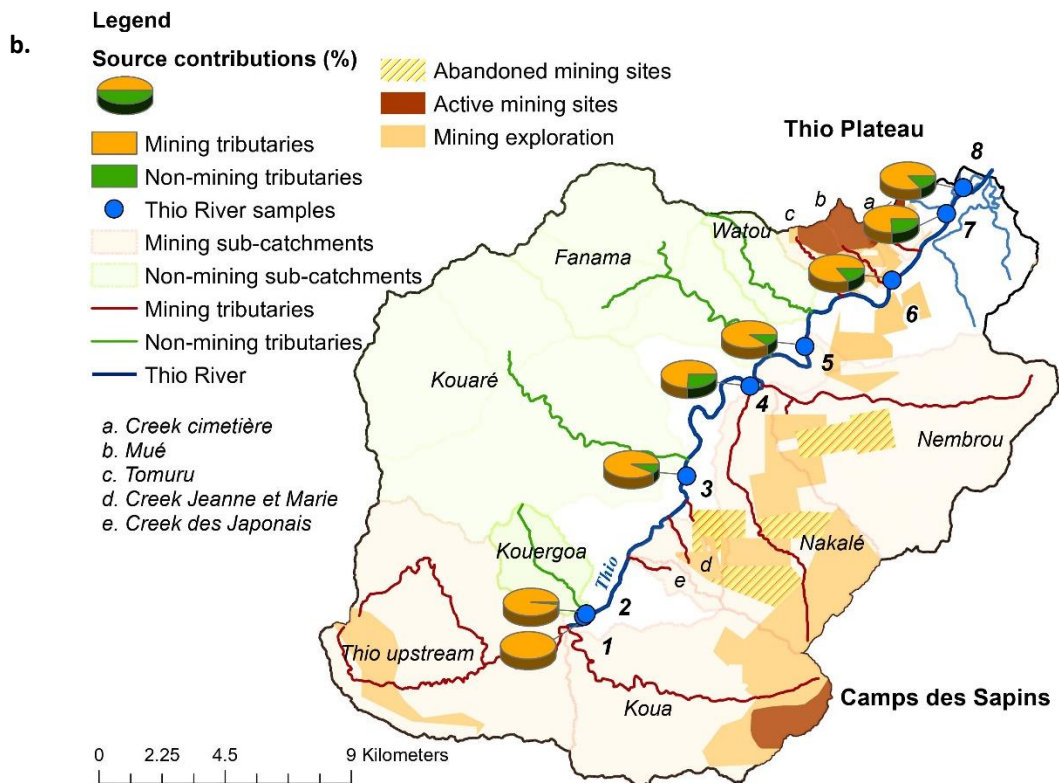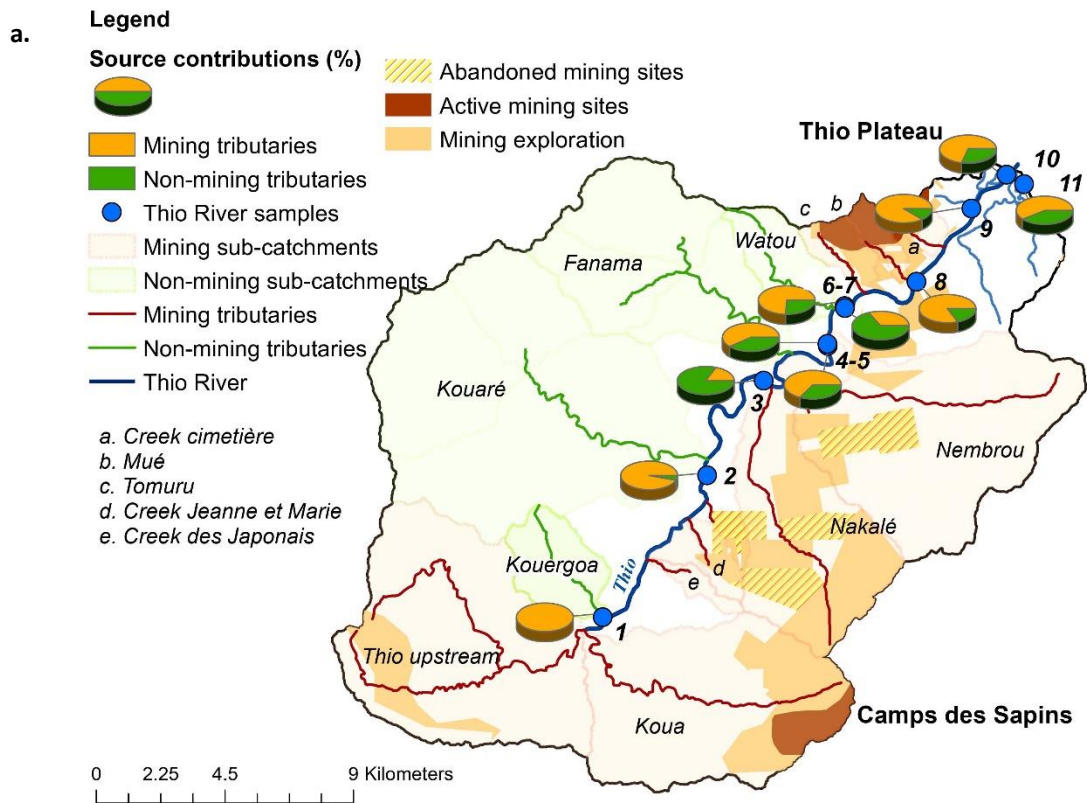
535   **Figure 9** Relative contributions of mining and non-mining tributaries to the sediment collected in the Thio River

536   during the 2015 (a) and 2017 (b) flood events using the 'colour + geochemistry' model

3.5.3 FDVS-PLSR model

Unlike the conventional fingerprinting approach, the estimated contributions of sources were not limited to vary in the range between 0 % and 100 %. In a similar way, the sum of source contributions was not constrained to be equal to 100 %. As a result, another method ~~way~~ to control the reliability of predictions was to sum the predicted proportions of both models. ~~For example, if the sum of the source contributions is close to 100 ± 20% then~~ and to verify that this sum was close to 100 % with an acceptable error of ± 20 %. If this point is not verified, ~~—~~ it is likely that a potential source has not been sampled and considered in the study or that the behaviour of the fingerprinting properties is not conservative (Legout et al., 2013). When applying the FDVS-PLSR models (i.e. mining and non-mining tributary contributions) to the river sediment samples (2015, 2017), the mean sums of the source contributions were 92 ± 8 % and 80 ± 13 %, respectively, for the 2015 and 2017 flood events (Tables 4 and 5) which are satisfactory results. However, for the 2017 flood events, three river sediment samples collected on sampling points n°1, 2 and 3 showed sums of source contributions below 70 %, indicating a lack of reliability of the model. The results obtained on these three points must therefore be interpreted with great caution. Moreover, and owing that predicted sums were slightly different from the expected 100 %, a bar plot display of the source contributions has been chosen to facilitate the interpretation of the results (Figure 10).

According to the FDVS-PLSR model results, 34 ± 22 % of sediment supply originated from mining tributaries while non-mining tributary contribution provided 58 ± 18 % of the sediment input for the 2015 flood event (Figure 10-a, Table 4). In the upper part of the Thio River catchment, non-mining tributaries largely dominated with a contribution of 80 % versus 6 % for mining tributaries. Along the Thio River, mining tributary contributions gradually increased to reach 70 % after the Mué tributary confluence (i.e. one of tributaries draining the Thio Plateau Mine, Figure 8-a, Table 4, sampling point [9]). The non-mining tributary contributions fluctuated along the Thio River between 41-85 % (Figure 8-a, Table 4, sampling points [2-8]) and reached a minimum to 28 % (Figure 10-a, Table 4, sampling point [9]) after the Mué tributary confluence. In the estuary, sediment supply was

563   originated from 51-70 % of mining tributaries and 28-52 % of non-mining tributaries (Figure 10-a,

564   Table 4, sampling points [9, 10, 11]).

565   The FDVS-PLSR models also indicated that mining and non-mining tributaries respectively

566   contributed a mean of 29 ± 20 % and 51 ± 11 % of sediment (Figure 10-b, Table 5) during the 2017

567   flood event. In a similar way, mining contributions gradually increased along the Thio River from 11 %

568   in upper parts to reach 52-58 % in the estuary. On the contrary, non-mining contributions gradually

569   decreased from 56 % in uppermost parts to reach 35-36 % in the estuary (Figure 10-b, Table 5).

570   In summary, the FDVS-PLSR models provided opposite results to those of the conventional

571   sediment fingerprinting approach (i.e. 'geochemistry' and 'colour + geochemistry' models). According

572   to the FDVS-PLSR models, non-mining tributaries contributed the majority of the sediment supply for

573   the 2015 (58 ± 18 %) and 2017 (51 ± 11 %) flood events. On the contrary, the 'geochemistry' and

574   'colour + geochemistry' models demonstrated that mining tributary contributions dominated

575   sediment supply for the 2015 (i.e. respectively 65 ± 27 % and 68 ± 28 %) and 2017 flood events (i.e.

576   respectively 83 ± 8% and 88 ± 8%).

577

578

579

580
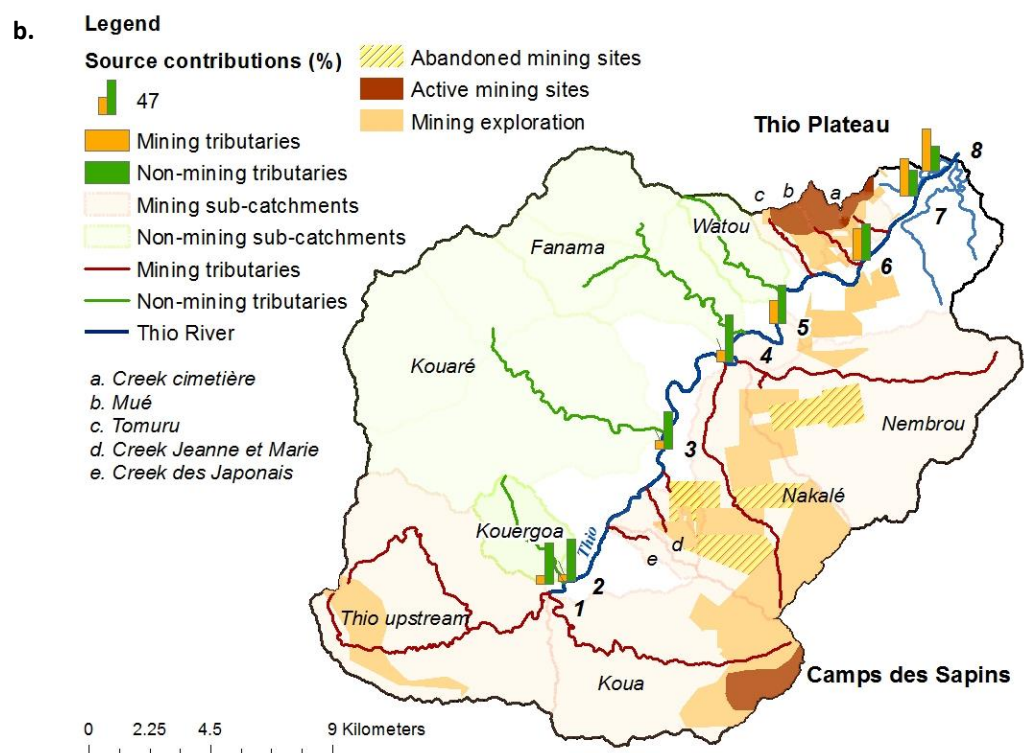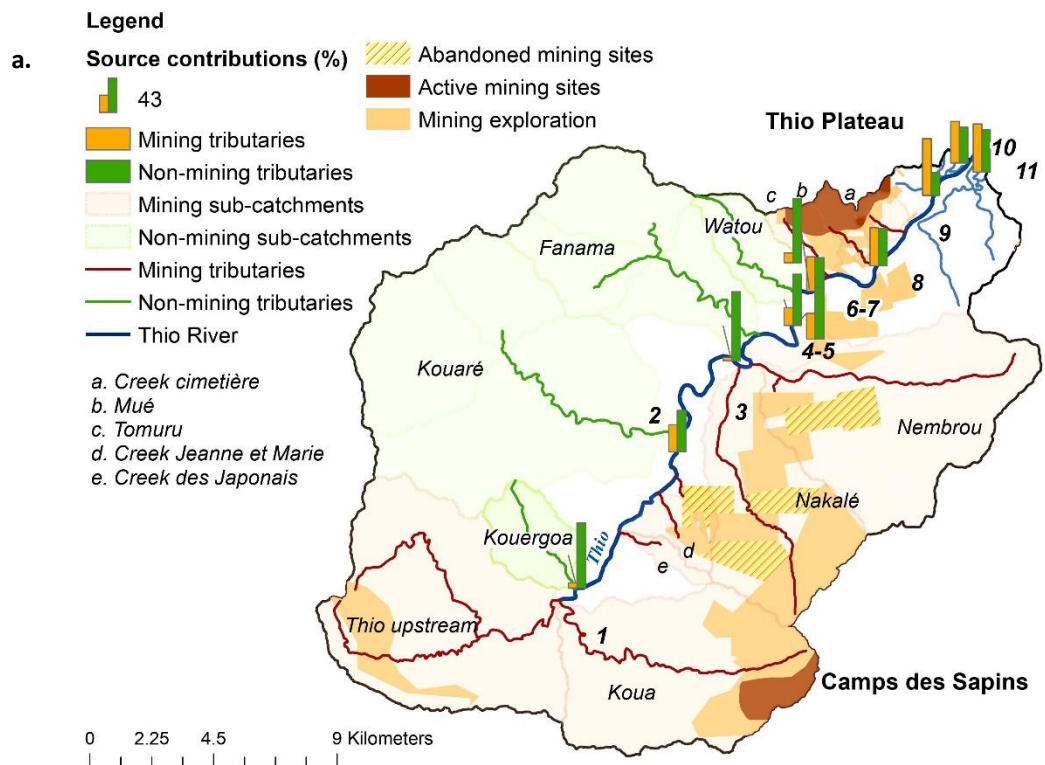
581 **Figure 10** Relative contributions of mining and non-mining tributaries to the sediment collected in the Thio

582   River during the 2015 (a) and 2017 (b) flood events using the FDVS-PLSR models

583   **Table 4** Source contributions calculated by FDVS-PLSR, 'geochemistry', 'colour + geochemistry' approaches for sediment deposited during the flood of February 25, 2015

584   (Mean, SD: standard deviation, minimum, maximum)

Sampling point	Mining tributary contributions (%)			Non-mining tributary contributions (%)			Sum of source contributions (%)		
	FDVS- PLSR	Geochemistry	Colour + Geochemistry	FDS- PLSR	Geochemistry	Colour + geochemistry	FDS- PLSR	Geochemistry	Colour + geochemistry
1	6	96	99	80	4	1	86	100	100
2	33	95	96	51	5	4	84	100	100
3	4	17	17	85	83	83	90	100	100
4	32	65	65	64	35	35	96	100	100
5	22	41	59	63	59	41	85	100	100
6	42	77	74	41	23	26	83	100	100
7	12	29	34	79	71	66	91	100	100
8	47	85	83	46	15	17	93	100	100
9	70	88	89	28	12	11	98	100	100
10	51	64	70	44	36	30	94	100	100
11	59	60	58	52	40	42	111	100	100
Mean (%)	34	65	68	58	35	32	92	100	100
SD (%)	22	27	25	18	27	25	8	-	-
Minimum (%)	4	17	17	28	4	1	84	-	-
Maximum (%)	70	96	99	85	83	83	111	-	-

588 **Table 5** Source contributions calculated by FDVS-PLSR, 'geochemistry', 'colour + geochemistry' approaches for sediment deposited during the flood of April 10,2017 (Mean,

589 SD: standard deviation, minimum, maximum)

Sampling point	Mining tributary contributions (%)			Non-mining tributary contributions (%)			Sum of source contributions (%)		
	FDVS-PLSR	Geochemistry	Colour + Geochemistry	FDS- PLSR	Geochemistry	Colour + geochemistry	FDS- PLSR	Geochemistry	Colour + geochemistry
1	11	90	100	56	10	0	66	100	100
2	9	94	98	58	6	2	68	100	100
3	11	89	92	52	11	8	63	100	100
4	16	69	74	66	31	26	82	100	100
5	32	82	89	54	18	11	86	100	100
6	44	81	84	51	19	16	95	100	100
7	52	77	83	36	23	17	88	100	100
8	58	83	85	35	17	15	92	100	100
Mean (%)	29	83	88	51	17	12	80	100	100
SD (%)	20	8	8	11	8	8	13	-	-
Minimum (%)	9	69	74	35	6	0	63	-	-
Maximum (%)	58	94	100	66	31	26	95	-	-

3.6 Complementary tests: representativeness of artificial mixture samples used for the FDVS-PLSR models compared to source samples

The FDVS-PLSR models provided contradictory results compared to those obtained with the 'geochemistry' and 'colour + geochemistry' models. In order to explain these results, complementary analyses were carried out with this model. This model was built from the mining and non-mining tributary samples (i.e. mixture of source samples > source poles > artificial mixture samples > FDVS-PLSR models). The objective of these analyses was to check whether the model is 'well built', in other words whether it is representative of the sources identified and whether it is capable of correctly 'classifying' the sources. To this end, we applied the FDVS-PLSR models on source samples to estimate their composition in terms of source contributions with FDVS-PLSR models. In the same way as we did above for the river sediment samples, we assessed the reliability of predictions by summing the source contributions predicted by both models (Legout et al., 2013). A mean sum of the predicted source proportions of 94 ± 17 % was calculated from the source sample data set which again is an excellent result. However, for the three mining tributary samples collected on the Koua tributary, the corresponding sums remained below 65 % with a minimum of 49 % whereas for one of the non-mining tributary sample collected on the Kouaré tributary, the sum reached 131 % (Figure 11). These results indicate that the FDVS-PLSR models provide unreliable predictions when dealing with river sediment samples with a colour signature partly due to these four samples. The colorimetric signature of the mining tributary samples collected on the Koua tributary in particular is not fully recognized by the models. The compositions of mining and non-mining tributary samples in Figures 11 and 12 also show that artificial mixture samples built from a mix between the composite mining source sample and the composite non-mining source sample did not cover entirely the range of values found in all the sources samples which may explain why some source samples showed mining and non-mining tributary composition lower than 0 and/or higher than 100 %.
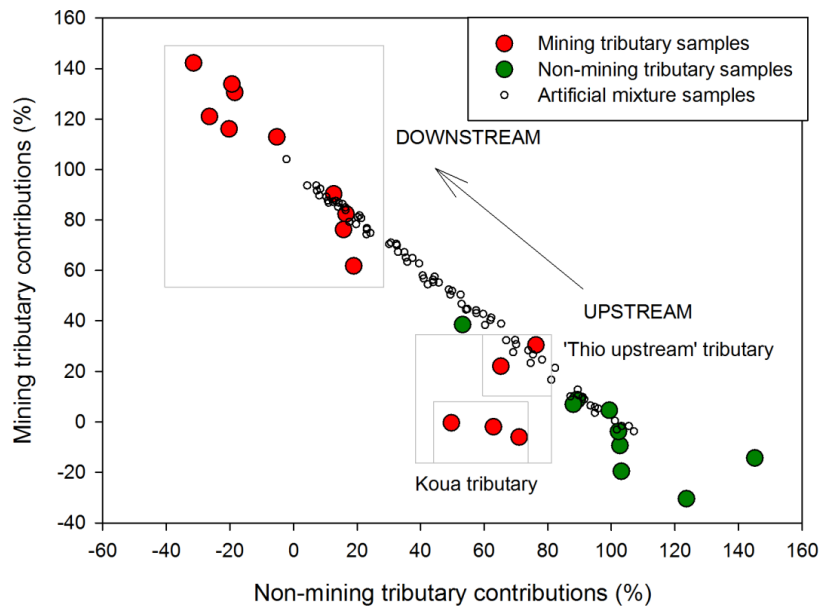
Figure 11 Relative compositions of mining and non-mining sources estimated by the FDVS-PLSR models applied to the individual source sediment samples

Moreover, we observed that two sub-groups of mining tributary samples can be distinguished, the first one corresponding to samples collected on the mining tributaries located in the uppermost part of the catchment and the second to samples collected on the mining tributaries located further downstream. The FDVS-PLSR differentiated rather well the second group since the mining tributary composition is dominant in these samples. On the contrary, the first group referred to as 'Upstream' merged with the non-mining tributary samples (Figure 11). Indeed, Figure 12 shows the mining tributaries located in the upper part of the catchment were defined as 'non-mining tributaries' by the FDVS-PLSR models.

624
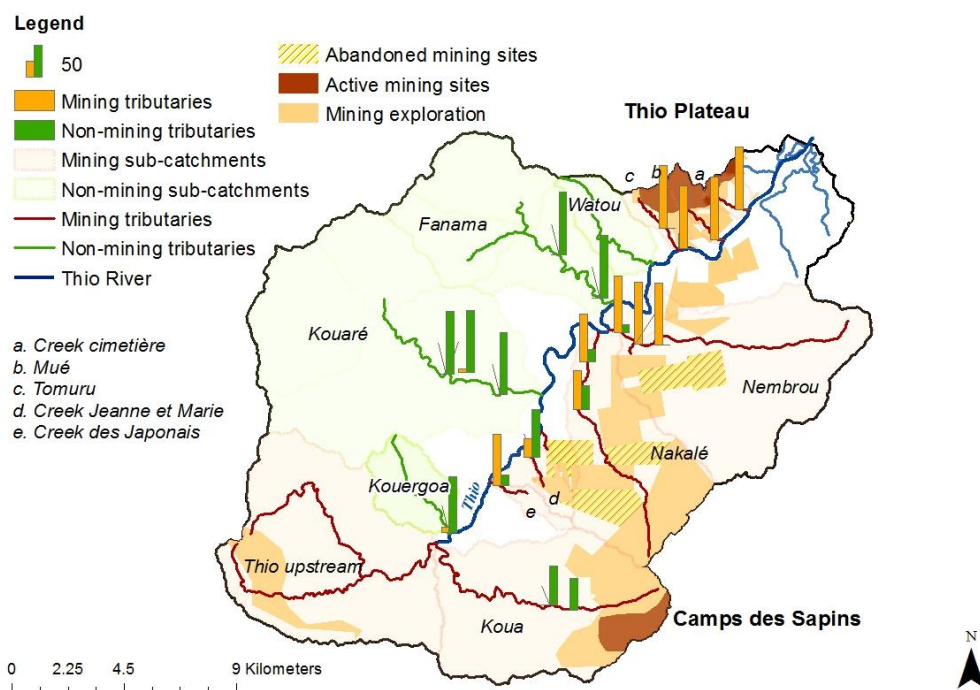
Figure 12 Relative compositions of mining and non-mining sources estimated by the FDVS-PLSR models applied to the individual sediment sources in the Thio River catchment

The low K contents found in these samples confirmed, however, that they were mainly supplied by mining sources (Figure 13). Indeed, only tributaries draining peridotite massifs (i.e. mining areas) can show such low K contents in source samples (Sellier et al., 2019). Nevertheless, a colour difference could be observed visually and through variations of the a* parameter: the a* values increased from upper parts to lower, which results in an increasingly red coloration of mining tributary samples in downstream direction. Figure 13 shows also that the a* values found in samples collected in the upper catchment part overlapped with those of non-mining tributary samples.
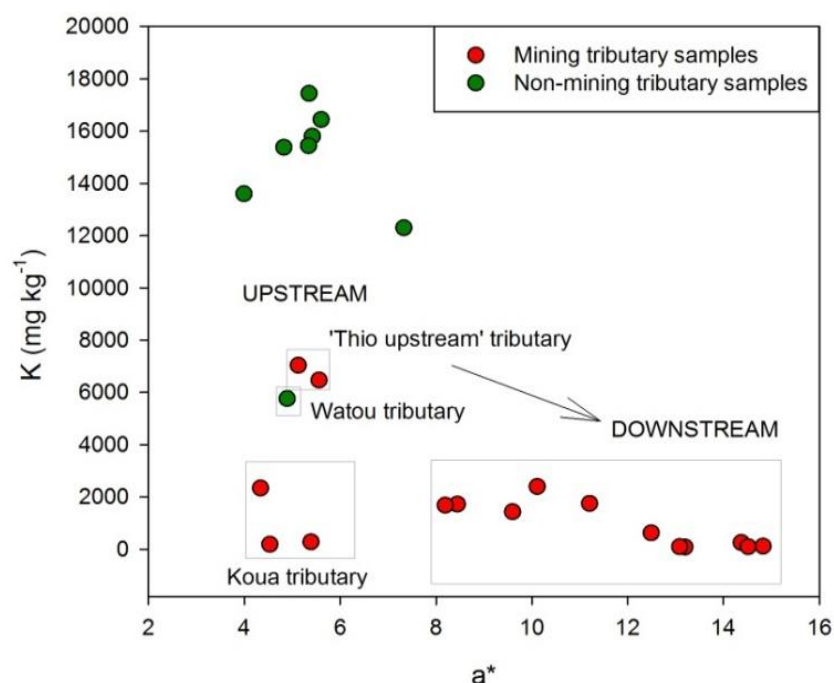
634   **Figure 13** Diagram of K contents as a function of a* parameter values within sediment sources and artificial

635   mixture samples

636   **4.Discussion**

637   **4.1 Advantages and limits of models**

638   4.1.1   'Colour' model

639   One of the objectives of this study was to test the contribution of spectrocolorimetry for

640   improving the source discrimination. Indeed, visual observations indicated that mining tributary

641   samples were red-orange whereas non-mining tributary samples were rather yellow-grey (Figure 1).

642   However, the results showed that the colour parameters, when used individually, did not provide

643   sufficient discrimination between sources (Table 2) to meet this objective. Indeed, some mining

644   tributary samples showed colour parameter values similar to those found in non-mining tributary

645   samples (e.g. v' at Table 3, or a* shown at Figure 13). This overlap of value ranges could explain in

646   particular the inability of the 'colour' model to provide satisfactory source discrimination. In the case

647   of mining sources, minerals such as hematite or goethite ~~provide them their~~ have a reddish-orange

648   colour (Quantin et al., 1997). Indeed, hematite is a red coloured oxidized mineral while goethite is a

649   yellow coloured oxidized mineral (Trescases, 1973). According to Figure 6, non-mining tributary

650   samples also have high contents of goethite which could interfere with the discrimination of the

651   colour signatures of the two sources. The non-mining tributaries drain areas devoid of mining

652   activities mainly located on the volcano-sedimentary formation rocks. The soil-geological profiles

653   within the volcano-sedimentary formation rocks are characterized at the surface by clay horizons and

654   at depth by oxidized horizons enriched in goethite in particular (Denis, 1988). According to Sellier et

655   al. (2019), subsurface erosion processes dominate in the Thio River catchment. In other words,

656   landslides mainly contribute to non-mining sediment inputs. As a result, the oxidized horizons of

657   these rock formations are also likely subject to erosion processes which could explain the occurrence

658   of goethite and material with a yellow-grey color in non-mining tributary samples.

659

660   Moreover, results obtained with colour parameter analyses coupled to visual observations

661   highlighted the occurrence of two groups of mining tributary samples (i.e. 'Upstream' and

662   'Downstream'). The coloration differences (i.e. orange/ 'Upstream' and 'red/Downstream') observed

663   between these two groups could be due to the the fact that on the one hand, the reddish colour

664   does not provide a highly conservative signature as it may be altered by the oxydo-reduction of iron

665   minerals during the periods of submersion of sediments under water. On the other hand, the

666   presence of different types of ~~nickel ores~~laterite profiles could explain these coloration differences.

667   Indeed, the laterite profile is classically described in the literature as composed of peridotites at the

668   bottom > saprolites > yellow laterites rich in goethite > red laterites rich in hematite at the top

669   (Trescases, 1973). However, certain minor features may be found in the laterite profile depending on

670   the type of parent rock found at the base of the peridotite massifs (Sevin, 2014). The mineral

671   composition found in the different layers of the laterite profile may vary depending on whether

672   serpentines or peridotites are the source rocks. Moreover, ~~nickel ore~~ laterite profile formation

673   depends partly on the morphological context, for instance on whether laterites~~nickel ores~~ are

674   located in a basin, on a plateau or a slope. This morphological context influences the weathering level

of peridotites and the formation of laterite profile: the more the laterite profile is altered, the higher

the thickness of red laterites. In the Thio River catchment, ~~nickel ores~~the laterite profile from the

Thio Plateau mine located in the downstream part of the catchment are 'plateau laterites~~nickel ores~~'

whereas those from the Camps des Sapins mine located in the upstream part of the catchment are

'slope laterites' ~~nickel ores'~~ (Mardhel et al., 2018). No information is provided in the literature on the

types of ~~nickel ores~~laterite profiles that were mined in abandoned mining sites. The red coloration of

the 'Downstream' mining tributary samples could then be associated with more altered laterite

profiles with a thicker layer of red laterites characteristic of 'plateau laterites~~nickel ores~~' compared to

the 'Upstream' mining tributary samples, which could be associated with a laterite profile with a

thinner layer of red laterites characteristic of 'slope laterites~~nickel ores~~'. The red laterites are the

final stage of alteration of the peridotite massifs. It therefore appears likely that the less altered

'slope laterites~~nickel ore~~' probably contain~~s~~ more yellow laterites enriched in goethite compared to

the 'plateau laterites~~nickel ore~~'. This hypothesis could explain the similar colour signature of the

mining tributary samples collected on the Koua tributary draining the Camps des Sapins mine and the

non-mining samples.

4.1.2 'Geochemistry' model

The 'geochemistry' model based on K provided significant discrimination between sources

(Table 2), regardless of the types of nickel ores that may be found in the Thio River catchment. K is a

lithological tracer discriminating sediments originating from the erosion of the two dominant

lithologies (i.e. peridotite massifs vs. volcano-sedimentary formations) in the Thio River catchment.

As anthropogenic erosion (i.e. due to mining activities) dominates on the peridotite massifs (Garcin

et al., 2017), K therefore provides an optimal discrimination between mining and non-mining

tributary contributions.

~~This~~ The parameter K classified the source samples rather well (i.e. 95.3 % of correct

classification, Table 3). Indeed, the 16 mining source samples were all correctly classified (100 %) and

only one non-mining source sample was not correctly classified (87.5 %); it corresponds to the Watou tributary sample (Figure 13). This sample showed a K content similar to that found in mining tributary samples. The Watou tributary is particular because it drains both volcano-sedimentary formations and peridotite massifs that were not exploited for mining, which justifies that it was considered as a non-mining tributary. The K content measured in this sample could be representative of that found in sediment sources characterized by a mix between the two dominant lithologies. Again, when observing Figure 13, two mining tributary samples (i.e. 'Thio upstream') showed similar K contents to that found in the Watou tributary sample. The 'Thio upstream' tributary also drains both areas associated with volcano-sedimentary formations and exploited peridotite massifs (i.e. mining prospection), which justifies that it was considered as a mining tributary.

The analysis of colour parameters coupled with that of geochemical elements indicated that these samples collected on the 'Thio upstream' tributary showed a less red coloration not because they are associated with a different type of ore, as could be the case for the samples collected on Koua tributary draining Camps des Sapins mine (Figure 13), but because they are characterized by a mix of both lithologies. As a result, the 'geochemistry' model showed a certain limitation to classify source samples characterized by a mix of both lithologies. The performance of the 'geochemistry' model described in Table 2 remains, however, excellent. The application of this model on artificial mixture samples provided very satisfactory results (Figure 5-a) with a good correlation between the predicted and the actual source proportions (r^2= 0.99). Estimations of mining tributary contributions may, however, be overestimated. This overestimation evaluated to a maximum at 15.5 % is greater when the mining contributions estimated by the model tend towards 0 % (maximum: 15.5 %, Figure 3-a). The 'geochemistry' model has difficulties to discriminate sediment contributions from sub-catchments with mixed lithologies. It classifies these types of samples as originating from mining tributaries, such as the Watou River sample. As a result, as the K concentrations decrease in the samples analyzed, the model will tend to overestimate the contributions of mining sources by default compared to their actual contributions.

726

727   4.1.3   'Colour + geochemistry' model

728   The 'colour + geochemistry' (i.e. K, Ca, Ti, b*, C*) model provided the best discrimination

729 between sources (Table 3). The inclusion of colour parameters in the 'colour + geochemistry'

730 approach allowed for the discrimination of source samples (i.e. 100 % of correctly classified source

731 samples) that a 'geochemistry' approach alone could not achieve. Results of the tests carried out on

732 the artificial mixture samples also showed an excellent correlation between the predicted and the

733 actual source proportions (i.e. r^2= 0.98). A slight overestimation of the mining tributary contributions

734 (7 %) was observed with this approach, which remains rather reasonable (Figure 3-b). In this model, K

735 is the lithological tracer which has the higher discriminant powerful (Table 2), which may explain the

736 similarity of results obtained with the 'colour + geochemistry' and the 'geochemistry' models.

737 Indeed, mining tributaries contributed an average of 65 ± 27 % for 'colour + geochemistry' model and

738 68 ± 25 % for 'geochemistry' model (Table 4). For the 2017 flood event, mining source contributions

739 largely dominated the sediment production with a mean contribution of 83 ± 8 % for the

740 'geochemistry' model and 88 ± 8 % for the 'colour + geochemistry' model.

741   4.1.4   FDVS-PLSR models

742   The FDVS-PLSR models built from artificial mixture samples showed excellent theoretical

743 predictive performances (e.g. r^2, RMSEC, RMSEC, Figure 7). However, the application of these models

744 on river sediment samples provided questionable results. Indeed, the artificial mixture samples did

745 not cover entirely the ranges of values found in all sources samples, thus resulting in an

746 overestimation (i.e. superior to 100 %) and an underestimation (i.e. inferior to 0 %) of source

747 composition (Figure 11) in several source samples. Similarly to what was previously observed, three

748 sub-groups of mining tributary samples can be distinguished, one of which (i.e. 'Thio Upstream') is

749 partially merged with the non-mining tributary samples (Figure 11). When modelling the source

750 contributions with the FDVS-PLSR models, a bias was created because the contributions of the 'Thio

751 upstream' tributary may be mainly considered as the contributions of non-mining tributaries. As a

752 result, an overestimation of non-mining tributary contributions may be found in the entire Thio River

753 catchment and particularly in the upper part of the study area. Third, the properties measured in the

754 Koua tributary (i.e. draining Camps des Sapins Mine) samples were not comprised in the ranges of

755 values covered by the artificial mixture samples (Figure 11).

756   Given the particular colour signature of this tributary (Figure 13), its contributions are

757 therefore not taken into account at all by the FDVS-PLSR models. Indeed, the sums of the source

758 contributions by FDVS-PLSR models are lower than the expected 100 % particularly in the uppermost

759 part of the catchment (Tables 4 and 5), which may indicate that a source is not accounted for.

760 Artificial mixtures were constructed from a homogenized spectral signature of all mining source

761 samples. However, two distinct spectral signatures were observed between the upstream and

762 downstream mining source samples. Homogenizing the spectral signature of the mining samples led

763 to a loss of information in terms of spectral signature, in particular that of the mining samples

764 located upstream. As a result, a 3-source FDVS-PLSR models (i.e. non-mining, upstream and

765 downstream mining sources) would have been more appropriate than 2-source FDVS-PLSR models in

766 this context.

767 **4.2 Spatial and temporal variations of sediment source contributions**

768   Among the four models tested in this study, the 'colour + geochemistry' model is the most

769 appropriate to estimate mining and non-mining tributary contributions in the Thio River catchment.

770 According to the results of this model, mining tributaries provided the main sediment supply to the

771 river system with a mean contribution of 68 ± 25 % for the 2015 flood event and 88 ± 8 % for the

772 2017 flood event (Tables 4 and 5). The variability of mining tributary contributions between these

773 two flood events with a return period of 10 years (3500 $m^3 s^{-1}$) could be explained in particular by the

774 variability of rainfall distribution (Sellier et al., 2019). Indeed, during the 2015 flood event, the Kouaré

775 River sub-catchment received twice the rainfall than observed in the rest of the Thio River

776 catchment, which may explain a higher contribution of non-mining tributaries for this event than for

777 the 2017 flood event where rainfall was more intense on the eastern part of the catchment in the

778 vicinity of the mines currently in operation (Thio Plateau, Camps des Sapins). In addition, the

779 inhabitants of Thio reported that bushfires had occurred in the Kouaré and Fanama sub-catchments

780 in 2015, which could have led to an increase in soil erosion processes, particularly landslides, in these

781 sub-catchments. This could also explain why the sediment contributions of the Kouaré tributary are

782 higher in 2015 compared to 2017. However, it is likely that, as for low intensity floods (i.e. <200 $m^3.s^-$

783 ^{1}), sediment generated during previous floods has been remobilized (Allenbach et al., 2020). The

784 current research does not allow to quantify this proportion of remobilized sediments. Future studies

785 based on the measurement of the $^7Be/^{210}Pb_{xs}$ ratio could provide information on this question as

786 both isotopes are supplied by rainfall and ^7Be is short-lived while $^{210}Pb_{xs}$ is much longer-lived. Indeed,

787 this ratio has been used in previous research to determine whether sediment has been eroded

788 recently (i.e. with a high ratio of $^7Be/^{210}Pb_{xs}$) or whether they have been remobilized from the

789 channel (i.e.with a low ratio of $^7Be/^{210}Pb_{xs}$) (Le Gall et al., 2017;Evrard et al., 2015).

790 Although the FDVS-PLSR models were unable to properly estimate the source contributions,

791 they provided qualitative indications about the proportion of sediment contribution between

792 'Upstream' and 'Downstream' mining tributaries at the level of the estuary. Indeed, only

793 'downstream' mining tributaries were finally identified by the FDVS-PLSR models as mining sources.

794 Mining contributions gradually increased in downstream direction. The predicted proportion sums of

795 river sediment samples also tend to reach the expected 100 %, which could result in a better

796 predictability of the models. As a result, these models indicated that sediment contribution from

797 downstream reaches dominated that of upstream reaches at the level of the estuary for both events.

798 Moreover, the analysis of colour parameters coupled to that of geochemical elements

799 highlighted the occurrence of three sub-groups of mining tributary samples, (1) 'Downstream'

800 samples characterized by high a* values and low K contents, (2) 'Koua tributary' samples located in

the upstream characterized by low a* values and low K contents and (3) 'Thio upstream' samples corresponding to a mix of both dominant lithologies (i.e. peridotite massifs and volcano-sedimentary formations) characterized by low a* values and higher K contents (i.e. 4 times higher than for the two previous sub-groups) (Figure 13). Owing to the low K contents found in Thio River sediment samples collected in the uppermost part (i.e. ~ 2200 mg kg^{-1} in 2015 and ~ 2600 mg kg^{-1} in 2017), which were similar to those measured in samples of sub-group (2) (~2400 mg kg^{-1}), it would appear that the Koua tributary draining Camps des Sapins mine dominated the sediment supply in the upstream for both events.

Conclusions

One of the objectives of this study was to evaluate the performance of sediment tracing methods based on spectroscopy measurements (i.e. colour parameters and FDVS). However, tThe results showed that these individual fingerprinting approaches based on spectroscopy did not provide sufficient discrimination between sources to be used for the modelling of sediment source contributions. Nevertheless, the inclusion of colour properties in addition to geochemical parameters turned out to be the optimal combination of tracers providing the highest discrimination between sediment sources. This 'colour + geochemistry' model is, however largely based on the discriminatory power provided by K, which explains why the results obtained between both models are so similar. Indeed, the contributions of mining tributaries were estimated to 65 ± 27 % by the 'colour + geochemistry' model versus 68 ± 25 % by the 'geochemistry' model for the 2015 flood event. In a similar way, the contributions of mining tributaries were estimated to 88 ± 8 % by the 'colour + geochemistry' model versus 83 ± 8 % by the 'geochemistry' model for the 2017 flood event. Moreover, both approaches have been experimentally validated. As a result, the use of these approaches could be extended to other mining catchments of New Caledonia but also possibly to other similar nickel mining areas (i.e. Ni oxidized ores based on peridotite massifs) around the world. In addition, although the individual fingerprinting approaches based on spectroscopy were not able

to discriminate sediment sources in the current research, spectroscopy measurements provided complementary information to that delivered by the geochemical properties alone to discriminate between sediment sources at the estuary. In the future, additional developments could be considered to improve this technique. The concept of a two-source sediment tracing approach (i.e. mining vs. non-mining tributary contributions) may be too simplistic in a mining context. The initial hypothesis that red-orange eroded sediment comes from mining tributaries whereas yellow-grey material originates from non-mining tributaries could not be fully confirmed in New Caledonia. Indeed, soils found in both mining and non-mining areas are all highly weathered and share similarities in terms of oxidized mineral composition (e.g. goethite), which likely generates confusion for discriminating their respective colorimetric signatures. Moreover, soils found across all mining areas across a single catchment are not necessarily identical, as different depths of their respective weathering profiles may crop out and result in variable colorimetric signatures. A preliminary identification of these soils characteristic of different weathering stages could be considered to improve the results of sediment tracing approaches based on spectroscopic measurements, both in New Caledonia and in other similar nickel mining catchments around the world.

~~means that the 'geochemistry' approach is also relevant to quantify sediment sources. Both approaches have, moreover, been experimentally validated. The current study showed that the contributions of mining sources dominated the sediment inputs with mean contributions of 68 % (SD 25 %) for the 2015 flood event and 88 % (SD 8 %) for the 2017 flood event (results of 'colour + geochemistry' model). Although the spatial variability of rainfall may impact local sediment source contributions, a trend in terms of sediment source contributions is observed along the Thio River for both flood events. In the uppermost part of the catchment, mining source contributions dominated (99% in 2015, 100% in 2017) with a dominant contribution from the Koua tributary draining the Camps des Sapins mine. The first non-mining tributary encountered in downstream direction (i.e. the Kouergoa tributary) contributed little to sediment supply; it is rather the next non-mining tributaries (i.e. the Kouaré tributary) which provided most of the sediment inputs (83 % in 2015, 26 % in 2017).~~

Nevertheless, these contributions were compensated in downstream direction by those from mining sources generated by tributaries draining Thio Plateau mine. Finally, at the estuary, mining sources dominated (58-70% in 2015, 83-85 % in 2017). These results therefore suggest that catchment management should focus on mining tributaries draining active mining sites (i.e. Camps des Sapins and the Thio Plateau).

As a result, the use of these approaches could be extended to other mining catchments of New Caledonia but alsoto other similar nickel mining catchments (i.e. Ni oxidized ores based on peridotite massifs) around the world.

Data availability

The database has been registered on the PANGEAE website and is currently undergoing the editorial process: https://issues.pangaea.de/browse/PDI-25229.

Author contribution

Oldrich Navratil, Michel Allenbach and Olivier Evrard designed research. Virginie Sellier, Oldrich Navratil, Olivier Evrard and Irène Lefèvre carried out fieldwork sampling. Virginie Sellier conducted the analyses. All co-authors contributed to data analysis and interpretation. John Patrick Laceby contributed to modelling. All co-authors contributed to the writing and approved the final version of the manuscript.

Competing interests

The authors declare that they have no conflict interest.

Acknowledgements

This work was funded by the National Technical Research Center (CNRT) "Nickel and Its Environment", Noumea, New Caledonia » (n°10PS2013-CNRT.UNC/IMMILA). The PhD project of

874 Virginie Sellier is also financed by the French Atomic Energy Commission (CEA, Commissariat à

875 l'Energie Atomique et aux Energies Alternatives). The authors are grateful to Jean-Guy M'Boueri,

876 Pierre Chanel, Jean-Jean, Lorenza M'Boueri, Nicolle Mathys for their invaluable support to identify

877 and have access to the field sampling sites. The authors would also like to thank Magdalena Uber for

878 her contribution to the spectrocolorimetric analyses.

879

880   **References**

881   Abel, A., Michael, A., Zartl, A., and Werner, F.: Impact of erosion-transported overburden dump
882   materials on water quality in Lake Cospuden evolved from a former open cast lignite mine
883   south of Leipzig, Germany, Environmental Geology, 39, 683-688, 2000.

884   Allenbach, M., Bertrand, M., Despinoy, Y., Evrard, O., Garcin, M., Liébault, F., Navratil, O., Recking, A.,
885   Richard, D., Rouet, I., Sabinot, C., Sellier, V., Tessier, B., Thinon, I., Touraivane, and Worliczek,
886   E.: Rapport scientifique. Programme « IMMILA, Impact de la mine au lagon ». CNRT « Nickel
887   & son environnement. 250 pages. , 2020.

888   Batista, P. V. G., Laceby, J. P., Silva, M. L. N., Tassinari, D., Bispo, D. F. A., Curi, N., Davies, J., and
889   Quinton, J. N.: Using pedological knowledge to improve sediment source apportionment in
890   tropical environments, J Soils Sediments, 10.1007/s11368-018-2199-5, 2018.

891   Baudrimont, M., Dominique, Y., Feurtet-Mazel, A., Gonzalez, P., Gourvès, P.-Y., Gunkel-Grillon, P.,
892   Laporte-Magoni, C., Lefrançois, E., Letourneur, Y., Marquié, J., Maury-Brachet, R., Monna, F.,
893   Pasquet, C., Rivière, E., and Roth, E.: - Rapport scientifique final. Programme « Dispersion des
894   métaux de la mine au lagon. ». CNRT « Nickel & son environnement ». 192 pages, 2019.

895   Bird, E. C. F., Dubois, J. P., and Iltis, J. A.: The impacts of opencast mining on the rivers and coasts of
896   New Caledonia. Tokyo, Japan, United Nations University, 1984.

897   Blake, W. H., Wallbrink, P. J., Wilkinson, S. N., Humphreys, G. S., Doerr, S. H., Shakesby, R. A., and
898   Tomkins, K. M.: Deriving hillslope sediment budgets in wildfire-affected forests using fallout
899   radionuclide tracers, Geomorphology, 104, 105-116, 10.1016/j.geomorph.2008.08.004, 2009.

900   Brosinsky, A., Foerster, S., Segl, K., and Kaufmann, H.: Spectral fingerprinting: sediment source
901   discrimination and contribution modelling of artificial mixtures based on VNIR-SWIR spectral
902   properties, Journal of soils and sediments, 14, 1949-1964, 2014.

903   Brown, A.: The potential use of pollen in the identification of suspended sediment sources, Earth
904   Surface Processes and Landforms, 10, 27-32, 1985.

905   Clarke, P., and David, C.: New Provincial Environmental Legislation in New Caledonia: Continuity and
906   Reform in Environmental Governance in a French Pacific Territory, Asia Pac. J. Envtl. L., 13,
907   135, 2010.

908   Collins, A., and Walling, D.: Selecting fingerprint properties for discriminating potential suspended
909   sediment sources in river basins, Journal of hydrology, 261, 218-244, 2002.

910   Collins, A. L., Walling, D. E., and Leeks, G. J. L.: Composite fingerprinting of the spatial source of fluvial
911   suspended sediment : a case study of the Exe and Severn river basins, United Kingdom,
912   Géomorphologie, 2, 41-53, 10.3406/morfo.1996.877, 1996.

913   Coulthard, T. J., and Macklin, M. G.: Modeling long-term contamination in river systems from
914   historical metal mining, Geology, 31, 451-454, 2003.

915   Danloux, J., and Laganier, R.: Classification et quantification des phénomènes d'érosion, de transport
916   et de sédimentation sur les bassins touchés par l'exploitation minière en Nouvelle Calédonie,
917   1991.

918   Daszykowski, M., Walczak, B., and Massart, D.: Representative subset selection, Analytica chimica
919   acta, 468, 91-103, 2002.

920   Davis, C. M., and Fox, J. F.: Sediment fingerprinting: review of the method and future improvements
921   for allocating nonpoint source pollution, J Environ Eng, 135, 490-504, 2009.

922   Debret, M., Sebag, D., Desmet, M., Balsam, W., Copard, Y., Mourier, B., Susperrigui, A.-S., Arnaud, F.,
923   Bentaleb, I., and Chapron, E.: Spectrocolorimetric interpretation of sedimentary dynamics:
924   the new "Q7/4 diagram", Earth-Science Reviews, 109, 1-19, 2011.

925   Denis, B.: Etude de sols fersiallitiques désaturés du plateau de Tango (Nouvelle-Calédonie), Cahiers
926   ORSTOM. Série Pédologie, 24, 61-76, 1988.

927   Dumas, P.: Méthodologie de cartographie de la sensibilité des sols à l'érosion appliquée à la région
928   de Dumbéa à Païta-Bouloupari (Nouvelle-Calédonie), Les Cahiers d'Outre-Mer. Revue de
929   géographie de Bordeaux, 63, 567-584, 2010.

930   Dumas, P., Printemps, J., Mangeas, M., and Luneau, G.: Developing erosion models for integrated
931   coastal zone management: A case study of The New Caledonia west coast, Marine Pollution
932   Bulletin, 61, 519-529, 2010.

933   Evrard, O., Laceby, J. P., Huon, S., Lefèvre, I., Sengtaheuanghoung, O., and Ribolzi, O.: Combining
934   multiple fallout radionuclides (137Cs, 7Be, 210Pbxs) to investigate temporal sediment source
935   dynamics in tropical, ephemeral riverine systems, J Soils Sediments, 16, 1130-1144,
936   10.1007/s11368-015-1316-y, 2015.

937   Evrard, O., Durand, R., Foucher, A., Tiecher, T., Sellier, V., Onda, Y., Lefèvre, I., Cerdan, O., and
938   Laceby, J. P.: Using spectrocolourimetry to trace sediment source dynamics in coastal
939   catchments draining the main Fukushima radioactive pollution plume (2011–2017), Journal
940   of Soils and Sediments, 1-12, 2019.

941   Evrard, O., Chaboche, P.-A., Ramon, R., Foucher, A., and Laceby, J. P.: A global review of sediment
942   source fingerprinting research incorporating fallout radiocesium (137Cs), Geomorphology,
943   107103, 2020.

944   Garcin, M.: Exploitation des granulats en lit vif des cours d'eau de la Grande-Terre, Nouvelle-
945   Calédonie. BRGM/RP-58531-FR. 114 p., 90 fig., 3 tabl., Bureau des Recherches Géologiques et
946   Minières 2010.

947   Garcin, M., Gastaldi, Y., and Lesimple, S.: Quantification et évolution temporelle des apports miniers
948   dans les rivières calédoniennes. BRGM/RP-66840-FR, 44 p., 23 fig., 5, Bureau des Recherches
949   Géologiques et Minières

950   2017.

951   Gruszowski, K., Foster, I. D., Lees, J., and Charlesworth, S.: Sediment sources and transport pathways
952   in a rural catchment, Herefordshire, UK, Hydrological Processes, 17, 2665-2681, 2003.

953   Hedouin, L., Pringault, O., Metian, M., Bustamante, P., and Warnau, M.: Nickel bioaccumulation in
954   bivalves from the New Caledonia lagoon: Seawater and food exposure, Chemosphere, 66,
955   1449-1457, 2007.

956   Highley, D., Chapman, G. R., and Bonel, K.: The economic importance of minerals to the UK, British
957   Geological Survey, 2004.

958   Iltis, J.: La mine, élement de la controverse écologique dans le Pacifique Sud, L'Espace géographique,
959   193-205, 1992.

960   James, L. A.: Legacy sediment: definitions and processes of episodically produced anthropogenic
961   sediment, Anthropocene, 2, 16-26, 2013.

962   Juillot, F.: – Rapport scientifique final. Programme « Dynamique des métaux de la mine au lagon ».
963   CNRT « Nickel & son environnement ». 202 pages., 2019.

964   Klages, M., and Hsieh, Y.: Suspended Solids Carried by the Gallatin River of Southwestern Montana:
965   II. Using Mineralogy for Inferring Sources 1, Journal of Environmental Quality, 4, 68-73, 1975.

966   Kumar, A., and Maiti, S. K.: Assessment of potentially toxic heavy metal contamination in agricultural
967   fields, sediment, and water from an abandoned chromite-asbestos mine waste of Roro hill,
968   Chaibasa, India, Environmental earth sciences, 74, 2617-2633, 2015.

969   Laceby, J. P., and Olley, J.: An examination of geochemical modelling approaches to tracing sediment
970   sources incorporating distribution mixing and elemental correlations, Hydrol. Process., 29,
971   1669-1685, 10.1002/hyp.10287, 2015.

972   Laceby, J. P., Evrard, O., Smith, H. G., Blake, W. H., Olley, J. M., Minella, J. P. G., and Owens, P. N.: The
973   challenges and opportunities of addressing particle size effects in sediment source
974   fingerprinting: A review, Earth-Sci. Rev., 169, 85-103, 10.1016/j.earscirev.2017.04.009, 2017.

975   Le Gall, M., Evrard, O., Foucher, A., Laceby, J. P., Salvador-Blanes, S., Manière, L., Lefèvre, I., Cerdan,
976   O., and Ayrault, S.: Investigating the temporal dynamics of suspended sediment during flood
977   events with 7 Be and 210 Pb xs measurements in a drained lowland catchment, Scientific
978   reports, 7, 42099, 2017.

979   Legout, C., Poulenard, J., Nemery, J., Navratil, O., Grangeon, T., Evrard, O., and Esteves, M.:
980   Quantifying suspended sediment sources during runoff events in headwater catchments
981   using spectrocolorimetry, J   Soils Sediments, 13, 1478-1492, 10.1007/s11368-013-0728-9,
982   2013.

983   Mardhel, V., Iseppi, M., Regninger, P. A., and Sevin, B.: Connaissance de l'ophiolite, géophysique
984   aéroportée et étude de la structure. Rapport scientifique final. Programme «OPHIOSTRUCT».
985   CNRT «Nickel & son environnement», 2018.

986   Martínez-Carreras, N., Udelhoven, T., Krein, A., Gallart, F., Iffly, J. F., Ziebel, J., Hoffmann, L., Pfister,
987   L., and Walling, D. E.: The use of sediment colour measured by diffuse reflectance
988   spectrometry to determine sediment sources: application to the Attert River catchment
989   (Luxembourg), J Hydrol, 382, 49-63, 2010.

990   Motha, J., Wallbrink, P., Hairsine, P., and Grayson, R.: Unsealed roads as suspended sediment sources
991   in an agricultural catchment in south-eastern Australia, Journal of Hydrology, 286, 1-18,
992   2004.

993   Navratil, O., Evrard, O., Esteves, M., Legout, C., Ayrault, S., Némery, J., Mate-Marin, A., Ahmadi, M.,
994   Lefèvre, I., and Poirel, A.: Temporal variability of suspended sediment sources in an alpine

995 catchment combining river/rainfall monitoring and sediment fingerprinting, Earth Surface
996 Processes and Landforms, 37, 828-846, 2012.

997 Owens, P. N., and Walling, D. E.: The phosphorus content of fluvial sediment in rural and
998 industrialized river basins, Water Res., 36, 685-701, 2002.

999 Pascal, N.: Ecosystèmes coralliens de Nouvelle-Calédonie. Valeur économique des services
1000 écosystémiques. Partie I: Valeur financière. IFRECOR., 2010.

1001 Poulenard, J., Perrette, Y., Fanget, B., Quetin, P., Trevisan, D., and Dorioz, J.-M.: Infrared
1002 spectroscopy tracing of sediment sources in a small rural watershed (French Alps), Science of
1003 the Total Environment, 407, 2808-2819, 2009.

1004 Poulenard, J., Legout, C., Nemery, J., Bramorski, J., Navratil, O., Douchin, A., Fanget, B., Perrette, Y.,
1005 Evrard, O., and Esteves, M.: Tracing sediment sources during floods using Diffuse Reflectance
1006 Infrared Fourier Transform Spectrometry (DRIFTS): A case study in a highly erosive
1007 mountainous catchment (Southern French Alps), Journal of Hydrology, 414, 452-462, 2012.

1008 Priadi, C., Ayrauk, S., Pacini, S., and Bonte, P.: Urbanization impact on metals mobility in riverine
1009 suspended sediment: role of metal oxides, International Journal of Environmental Science &
1010 Technology, 8, 1-18, 2011.

1011 Prior, T., Daly, J., Mason, L., and Giurco, D.: Resourcing the future: Using foresight in resource
1012 governance, Geoforum, 44, 316-328, 2013.

1013 Quantin, P., Bourdon, E., and Becquer, T.: Minéralogie et contraintes édaphiques des sols"
1014 ferritiques" dérivés de roches ultrabasiques en Nouvelle-Calédonie: relations entre
1015 constituants minéraux et disponiblté en certains éléments (Al, Fe, Si, Mg, Mn, Ni, Co, Cr, Cu,
1016 Zn, Mo) facilement solubles, 1997.

1017 Rossel, R. V., Walvoort, D., McBratney, A., Janik, L. J., and Skjemstad, J.: Visible, near infrared, mid
1018 infrared or combined diffuse reflectance spectroscopy for simultaneous assessment of
1019 various soil properties, Geoderma, 131, 59-75, 2006.

1020 Sellier, V., Navratil, O., Laceby, J. P., Allenbach, M., Lefèvre, I., and Evrard, O.: Investigating the use of
1021 fallout and geogenic radionuclides as potential tracing properties to quantify the sources of
1022 suspended sediment in a mining catchment in New Caledonia, South Pacific, Journal of Soils
1023 and Sediments, 1-17, 2019.

1024 Sevin, B.: Cartographie du régolithe sur formation ultrabasique de Nouvelle-Calédonie: Localisation
1025 dans l'espace et le temps des gisements nickélifères, Nouvelle Calédonie, 2014.

1026 Shellberg, J., Brooks, A., and Spencer, J.: Land-use change from indigenous management to cattle
1027 grazing initiates the gullying of alluvial soils in northern Australia, 19th World Congress of Soil
1028 Science: Soil Solutions for a Changing World, 2010, 1-6,

1029 Sherriff, S. C., Franks, S. W., Rowan, J. S., Fenton, O., and Ó'hUallacháin, D.: Uncertainty-based
1030 assessment of tracer selection, tracer non-conservativeness and multiple solutions in
1031 sediment fingerprinting using synthetic and field data, J Soils Sediments, 15, 2101-2116,
1032 10.1007/s11368-015-1123-5, 2015.

1033 Smith, H. G., Sheridan, G. J., Lane, P. N. J., Noske, P. J., and Heijnis, H.: Changes to sediment sources
1034   following wildfire in a forested upland catchment, southeastern Australia, Hydrol. Process.,
1035   25, 2878-2889, 10.1002/hyp.8050, 2011.

1036 Surell, A.: Étude sur les torrents des Hautes-Alpes, Carilian-Goeury, 1841.

1037 Tiecher, T., Caner, L., Minella, J. P., and dos Santos, D. R.: Combining visible-based-color parameters
1038   and geochemical tracers to improve sediment source discrimination and apportionment, Sci
1039   Total Environ, 527-528, 135-149, 10.1016/j.scitotenv.2015.04.103, 2015.

1040 Trescases, J. J.: Weathering and geochemical behaviour of the elements of ultramafic rocks in New
1041   Caledonia, BMRJ. Aust. Geol and Geophys., 141, 149-161, 1973.

1042 Uber, M., Legout, C., Nord, G., Crouzet, C., Demory, F., and Poulenard, J.: Comparing alternative
1043   tracing measurements and mixing models to fingerprint suspended sediment sources in a
1044   mesoscale Mediterranean catchment, Journal of Soils and Sediments, 1-19, 2019.

1045 Valette-Silver, N. J.: The use of sediment cores to reconstruct historical trends in contamination of
1046   estuarine and coastal sediments, Estuaries, 16, 577-588, 1993.

1047 Varol, M.: Assessment of heavy metal contamination in sediments of the Tigris River (Turkey) using
1048   pollution indices and multivariate statistical techniques, Journal of Hazardous Materials, 195,
1049   355-364, 2011.

1050 Wallbrink, P., Murray, A., Olley, J., and Olive, L.: Determining sources and transit times of suspended
1051   sediment in the Murrumbidgee River, New South Wales, Australia, using fallout 137Cs and
1052   210Pb, Water Resour Res, 34, 879-887, 1998.

1053 Wallbrink, P. J.: Quantifying the erosion processes and land-uses which dominate fine sediment
1054   supply to Moreton Bay, Southeast Queensland, Australia, Journal of environmental
1055   radioactivity, 76, 67-80, 2004.

1056 Walling, D., Peart, M., Oldfield, F., and Thompson, R.: Suspended sediment sources identified by
1057   magnetic measurements, Nature, 281, 110, 1979.

1058 Yellishetty, M., Mudd, G. M., and Shukla, R.: Prediction of soil erosion from waste dumps of opencast
1059   mines and evaluation of their impacts on the environment, International Journal of Mining,
1060   Reclamation and Environment, 27, 88-102, 2013.

1061